A Quest to Fluid Stress Tensor, Part II: Can We Solve the Conflicts?

Wanan Sheng [1,2]

[1] Department of Aerospace and Mechanical Engineering, South East Technological University, Carlow, R93 V960, Ireland
[2] SW MARE Technology Ireland
* Correspondence: wanan.sheng@setu.ie

Abstract: The symmetric stress tensor (SST) is widely used in the constitutive description of Newtonian fluids. This manuscript examines the author's proposed objections to that description and compares it with an asymmetric stress tensor (AST). The discussion considers the derivation of the Navier–Stokes momentum equation, spatial stress increments, planar Poiseuille flow, wall traction, drag and lift on a sphere, rigid-body rotation, and compressible viscous dissipation. The proposed AST reproduces selected momentum and drag expressions under the stated assumptions, while giving different individual stress components and stress-power terms. A proposed decomposition of mechanical power is also examined for rotating and dilatational velocity fields. The interpretation of these comparisons requires several distinctions: stress symmetry is local and does not imply spatial uniformity; complementary tensor components are not automatically separate forces on the same wall; the sphere-force calculation requires a complete surface projection; and zero dissipation under Stokes' hypothesis depends on the selected deformation field and bulk-viscosity assumption. The discussion therefore distinguishes the author's proposed constitutive interpretation from conclusions that follow directly from the displayed algebra. Particular attention is given to the difference between viscous-force power, stress-work transport, and conversion to internal energy. The unresolved requirements include consistent tensor indexing, angular-momentum balance, observer invariance, and thermodynamic admissibility. The manuscript presents a theoretical comparison rather than experimental validation of an alternative fluid law. The equations and illustrative configurations are retained to make the proposal assessable, while claims that the AST resolves every alleged conflict are qualified by the additional physical conditions that would be necessary to support such a conclusion.

Keywords: Newton's law of viscosity; viscous stress tensor; symmetric stress; asymmetric stress; Navier–Stokes equations; mechanical power; viscous dissipation

Citation: Sheng, W. 2026. A Quest to Fluid Stress Tensor, Part II: Can We Solve the Conflicts? *TK Techforum Journal (ThyssenKrupp Techforum)* 2026(4): 49–82.
https://doi.org/10.71448/tk202644

Received: 10-Sep-2026
Revised: 20-Oct-2026
Accepted: 24-Oct-2026
Published: 07-Nov-2026

Copyright: © 2026 by the authors. Licensee TK Techforum Journal (ThyssenKrupp Techforum). This article is an open access article distributed under the terms and conditions of the Creative Commons Attribution (CC BY) license (https://creativecommons.org/licenses/by/4.0/).

1. Introduction

The symmetric stress tensor (SST) has played a central role in descriptions of fluid viscous stress since the early formulations of the equations of motion associated with Navier (1827), Cauchy (1828), Poisson (1831), Saint-Venant (1843), and Stokes (1845). Later contributions included work by Maxwell, Kirchhoff, and Boltzmann [1]. In particular, the formulation developed by Stokes became part of the standard treatment presented in fluid-mechanics and aerodynamics textbooks [2–8].

Historical investigations also considered nonsymmetric viscous stresses, particularly during the 1960s [9–12]. Van D'en and Listrov [12] discussed earlier studies of fluid models with asymmetric stress tensors, while Listrov [11] examined a viscous-fluid model without the conventional symmetry restriction. These contributions should be distinguished from the classical Newtonian-fluid model and from the subsequent development of turbulence modeling and computational fluid dynamics (CFD) [13–17]. More recently, Sheng [18] proposed an asymmetric stress tensor (AST) and argued that it could reproduce the

Navier–Stokes (N–S) momentum equation while resolving perceived inconsistencies in the interpretation of Couette flow.

The proposed AST challenges a longstanding constitutive description and therefore requires careful examination of its assumptions, balance laws, and physical implications. Following publication of the earlier proposal [18], Natarajan and Natarajan published a critique [19]. The present author disputes aspects of their coordinate-based calculation, which are discussed later in this manuscript. Luo subsequently examined stress-tensor symmetry in gas flows, including the role of internal moments and the assumptions entering angular-momentum balance [20]. That work provides relevant theoretical context, but it should not be treated as experimental confirmation of every claim made for the AST considered here.

The present study develops the author's arguments through several illustrative flow configurations, building on the preceding manuscript [21]. The proposed objections concern seven main issues: (1) whether the stress equalities imposed on a finite fluid element would imply a spatially uniform stress field and prevent the derivation of viscous-force terms; (2) the interpretation of wall shear stress and its relation to flow separation; (3) the calculation of lift on a sphere in an axisymmetric flow; (4) the treatment of stress increments in planar Poiseuille flow; (5) the claimed dependence of stress derivatives on the element aspect ratio; (6) stresses, energy transfer, and dissipation during rigid-body rotation; and (7) the interpretation of zero dissipation in a particular compressible velocity field. These are the author's proposed objections to the conventional formulation, rather than established consequences of stress symmetry.

The discussion addresses two related questions: how the author interprets the practical success of calculations based on symmetric stress, and what changes when the proposed asymmetric relation is used instead. The examples compare force calculations, momentum equations, and energy expressions. The purpose is to make the proposed reasoning explicit, including its assumptions and its remaining unresolved points, so that the competing interpretations can be assessed on the basis of their mathematical definitions and physical balance laws.

The manuscript is organized as follows. Section 2 introduces the total stress tensor and the conventional symmetric viscous-stress relation. Section 3 presents the author's objections through momentum-balance, wall-traction, sphere-flow, rigid-rotation, and compressibility examples. Section 4 introduces the proposed AST and derives its contribution to the momentum equation. Section 5 revisits the stress-increment and planar Poiseuille-flow arguments. Section 6 applies the AST to the sphere-force calculation. Section 7 examines mechanical energy, stress power, and the proposed separation of transfer and dissipation. Section 8 considers the compressible-flow expression, and Section 9 summarizes the proposed interpretation and its unresolved requirements. The appendix sets out the polar-coordinate calculation used in the main text.

The comparison is theoretical and uses prescribed velocity fields rather than new measurements. The illustrations identify elements, coordinate directions, and force components; they do not constitute independent experimental evidence. Each example is therefore read at three levels: the definition of the tensor, the differentiation or integration performed on it, and the physical interpretation assigned to the result. Agreement at one level does not automatically establish agreement at the others. In particular, a field with zero stress divergence can still have nonzero stress, and a field with nonzero stress can transmit different boundary tractions depending on the chosen normal. Similarly, a vanishing bulk force term does not imply a vanishing mechanical-power flux. Keeping these distinctions explicit makes the proposed alternative easier to examine without confusing an algebraic identity with a constitutive law or an experimentally established mechanism. The remaining discussion retains the source equations and example sequence while specifying the assumptions that are needed to interpret them. Any claim of general validity must ultimately apply to the complete tensor field, the appropriate boundary conditions, and all relevant balances, rather than to a selected scalar component alone.

2. General and Symmetric Stress Tensors for Fluids

For completeness, this section introduces the total fluid stress, its viscous contribution, and the conventional symmetric constitutive expression used in the comparisons that follow.

2.1. General Fluid Stress Tensor

The total stress tensor $\vec{\vec{T}}$ for a three-dimensional flow is a second-order tensor. Double arrows denote tensor quantities throughout this manuscript. The pressure and viscous contributions are written separately as

$$\vec{\vec{T}} = \begin{bmatrix} -p & 0 & 0 \\ 0 & -p & 0 \\ 0 & 0 & -p \end{bmatrix} + \vec{\vec{\sigma}}, \tag{1}$$

where p is the fluid pressure and $\vec{\vec{\sigma}}$ is the complete viscous-stress tensor, including the volumetric contribution. Following the notation adopted from [3], it is expressed as

$$\vec{\vec{\sigma}} = \begin{bmatrix} \tau_{11} & \tau_{12} & \tau_{13} \\ \tau_{21} & \tau_{22} & \tau_{23} \\ \tau_{31} & \tau_{32} & \tau_{33} \end{bmatrix} + \begin{bmatrix} \lambda\nabla\cdot\vec{V} & 0 & 0 \\ 0 & \lambda\nabla\cdot\vec{V} & 0 \\ 0 & 0 & \lambda\nabla\cdot\vec{V} \end{bmatrix}, \tag{2}$$

where τ_{ij}, with $i, j = 1, 2, 3$, denotes the components of the viscous-stress contribution considered separately from the volumetric term; λ is the second viscosity coefficient; and $\vec{V}$ is the velocity vector. The scalar $\nabla \cdot \vec{V}$ is the velocity divergence. This notation makes the volumetric contribution explicit and allows the subsequent comparison to distinguish it from the remaining components.

The following discussion considers both the complete viscous-stress tensor $\vec{\vec{\sigma}}$ and the tensor $\vec{\vec{\tau}} = [\tau_{ij}]$. The proposed asymmetric relation is examined as an alternative constitutive description. Its physical interpretation must be assessed together with the definitions of traction, angular-momentum balance, and stress power, rather than from the component expressions alone.

2.2. Symmetric Stress Tensor (SST)

The standard symmetric viscous-stress relation described in the cited textbooks [2–8] has the following components:

$$\left.\begin{aligned} &\tau_{11} = 2\mu\left(\frac{\partial u_1}{\partial x_1}\right); \quad \tau_{22} = 2\mu\left(\frac{\partial u_2}{\partial x_2}\right); \quad \tau_{33} = 2\mu\left(\frac{\partial u_3}{\partial x_3}\right) \quad \text{- normal stresses,} \\ &\tau_{12} = \tau_{21} = \mu\left(\frac{\partial u_1}{\partial x_2} + \frac{\partial u_2}{\partial x_1}\right) \quad \text{- symmetric shear stresses,} \\ &\tau_{13} = \tau_{31} = \mu\left(\frac{\partial u_1}{\partial x_3} + \frac{\partial u_3}{\partial x_1}\right) \quad \text{- symmetric shear stresses,} \\ &\tau_{23} = \tau_{32} = \mu\left(\frac{\partial u_3}{\partial x_2} + \frac{\partial u_2}{\partial x_3}\right) \quad \text{- symmetric shear stresses,} \end{aligned}\right\} \tag{3}$$

Here x_i and u_i, with $i = 1, 2, 3$, are the spatial coordinates and velocity components, respectively. Thus, $(x_1, x_2, x_3) = (x, y, z)$ and $(u_1, u_2, u_3) = (u, v, w)$. The coefficient μ is the dynamic viscosity. The displayed components represent the part of the constitutive relation that is written separately from the second-viscosity term.

Compared with the simple-shear expression usually associated with Newton's law of viscosity, the general symmetric relation contains both cross derivatives. For example, $\partial u_1/\partial x_2$ and $\partial u_2/\partial x_1$ enter the same shear component. The author questions the interpretation of this pairing in the preceding manuscript [21]. In the conventional formulation, the pairing represents the symmetric part of the velocity gradient; it should therefore

be distinguished from an assumption that equal stress components have equal spatial derivatives in different directions.

Terminology is also important in this comparison. A nonsymmetric tensor is one that does not necessarily equal its transpose. An antisymmetric tensor, by contrast, equals the negative of its transpose and has zero diagonal components. These terms are not interchangeable. Some historical publication titles use the word antisymmetric, but that wording should not be taken to mean that the complete AST proposed here is purely antisymmetric. The matrix in Eq. (38) generally contains both symmetric and antisymmetric parts. The conventional rate-of-deformation tensor is the symmetric part of the velocity gradient, whereas the remaining part describes local rotation. A constitutive relation built from the complete gradient therefore responds differently to rigid-body rotation from one built from deformation alone. This distinction is present before any coordinate transformation is performed. It must remain visible when the same symbols are used in Cartesian, polar, and spherical-coordinate examples, because changing the basis does not change whether a properly defined tensor is symmetric at a particular physical point.

3. Why Does the SST Work in Practical Flow Calculations?

The preceding manuscript [21] questions the suitability of the SST for fluids, whereas the symmetric constitutive description has an extensive history of practical use. This section presents the author's interpretation of that apparent tension. The following five categories organize the proposed objections and identify the examples examined in detail. Their presentation does not by itself establish that conventional continuum mechanics requires the additional assumptions used in those objections.

1) Agreement in selected calculations. The author argues that the conventional derivation of the N–S equation and the calculation of Stokes drag contain steps that do not fully retain the stress interpretation being challenged. The AST is proposed as an alternative route to the same momentum equation and drag result. The sphere example is then used to examine a claimed discrepancy in lift. These comparisons require particular attention to whether the same traction definition is used in both calculations.

2) Interpretation of wall traction. The author questions whether the usual wall-shear expression and airfoil-force integrals include every component implied by a symmetric tensor. The argument concerns the distinction between a tensor component on a specified plane and the traction acting on the physical wall. The role of Newton's third law is discussed in that context, with the adopted surface-normal convention requiring explicit identification.

3) Stress increments and element dimensions. The planar Poiseuille-flow example is used to question the simultaneous equalities imposed at different positions on a fluid element. The author also examines a relation involving the element aspect ratio and interprets it as a possible source of grid dependence. These issues must be assessed at the level of the stated spatial assumptions.

4) Rigid-body rotation. The author distinguishes zero dissipation from a claim of zero stress-mediated energy transfer in a rotating configuration. The conventional Newtonian relation gives zero viscous stress for exact rigid-body rotation. The proposed counterexample introduces an applied torque and a resisting load, raising the additional question of whether exact rigid-body rotation remains dynamically admissible under those conditions.

5) Interpretation of dissipation. The author proposes describing viscous dissipation through relative deformation, termed sliding motion in this manuscript. Couette and planar Poiseuille flows are contrasted with rigid-body rotation. The latter has a nonzero velocity gradient but zero symmetric rate of deformation. The subsequent energy discussion examines the author's proposed decomposition while distinguishing a kinematic description from a thermodynamic justification.

The following subsections develop these arguments through explicit stress components, force expressions, and energy balances for the selected flow configurations.

3.1. On the Derivation of the N–S Equation

The conventional derivation of the N–S equation includes the divergence of viscous stress in the local momentum balance. The fluid element in Figure 1 illustrates the stress components and their first-order spatial increments. In the adopted notation, these increments are $\tau'_{13} = \tau_{13} + (\partial\tau_{13}/\partial x_3)\Delta x_3$ and $\tau'_{31} = \tau_{31} + (\partial\tau_{31}/\partial x_1)\Delta x_1$. Each expression compares a component at two nearby positions along its specified coordinate direction.

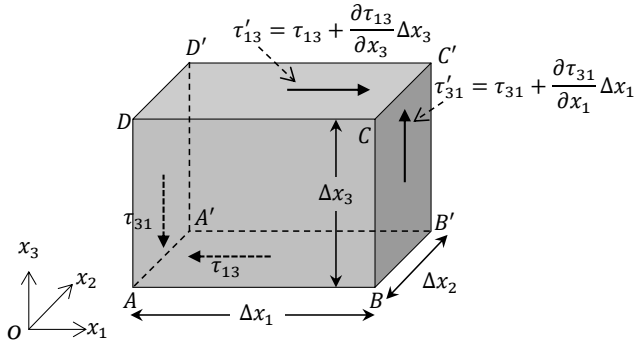


Figure 1. Fluid Element and Stress Components in the Momentum-Balance Construction

The argument below imposes the equalities $\tau_{13} = \tau_{31}$ and $\tau'_{13} = \tau'_{31}$ on the illustrated components. The intended purpose is to impose a moment condition about axes such as AA' and CC'. However, stress symmetry is a local statement at a common spatial point. Equalities between components evaluated at different face positions require an additional justification and must not be inferred from local symmetry alone.

Using the adopted index convention, the viscous-force density associated with the components τ_{ij} is written as

$$f_i^{vis} = \frac{\partial\tau_{ij}}{\partial x_j}. \tag{4}$$

Derivations of the viscous-force density are available in standard textbooks [3,22–24], while the preceding manuscript discusses the author's alternative interpretation [21]. Repeated indices are summed according to the Einstein convention. For example, $f_1^{vis} = \partial\tau_{11}/\partial x_1 + \partial\tau_{12}/\partial x_2 + \partial\tau_{13}/\partial x_3$. Corresponding expressions apply to f_2^{vis} and f_3^{vis}. The derivatives describe local spatial variations of the relevant stress components.

For a finite control volume, the surface-force balance involves the traction distributed over every face, together with body forces and the rate of momentum change. The pointwise differential equation follows from the limiting form of that balance. When moments are taken about a different origin, the resultant moment changes by the moment of the resultant force about the displacement between origins. Consequently, one cannot independently set every finite-element moment to zero while retaining arbitrary nonzero resultant forces and then infer new pairwise equalities between face stresses. The local angular-momentum condition and a separate finite-element static-equilibrium construction are different statements. This is why the position at which each component is evaluated matters in the argument. A diagram can suppress that distinction when all face labels are written without coordinates. In the present notation, primes should therefore be understood as identifying the stated displaced positions, not as a second tensor at an unspecified common point. That clarification is necessary before Eqs. (7a)–(8) can be interpreted as constraints on a continuum field.

For constant viscosity coefficients, the symmetric constitutive relation and Stokes' hypothesis, $\lambda = -2\mu/3$, give the following momentum equation for a compressible Newtonian fluid:

$$\rho\left(\frac{\partial u_i}{\partial t} + u_j\frac{\partial u_i}{\partial x_j}\right) = -\frac{\partial p}{\partial x_i} + f_{bi} + \mu\frac{\partial^2 u_i}{\partial x_j\partial x_j} + \frac{1}{3}\mu\frac{\partial}{\partial x_i}\left(\frac{\partial u_k}{\partial x_k}\right). \tag{5}$$

This equation includes the velocity-divergence contribution under the stated constitutive assumptions. The quantity f_{bi} denotes body force per unit volume. For an incompressible fluid with constant dynamic viscosity, the momentum equation reduces to

$$\rho\left(\frac{\partial u_i}{\partial t}+u_j\frac{\partial u_i}{\partial x_j}\right)=-\frac{\partial p}{\partial x_i}+f_{bi}+\mu\frac{\partial^2 u_i}{\partial x_j\partial x_j}. \tag{6}$$

Eqs. (5) and (6) are the conventional compressible and incompressible forms used here. Their applicability depends on the stated constitutive and material assumptions; they are not unrestricted descriptions of every possible fluid.

The derivation is presented in the cited textbooks [3,22–24]. The discussion below challenges the author's interpretation of the stress equalities entering a finite-element moment argument, rather than the algebraic operation of taking the stress divergence itself.

The author's argument:

The author's argument starts from the requirement that the illustrated shear stresses satisfy moment balance about selected axes. Taking CC' and AA' as reference axes is interpreted as giving $\tau_{13}=\tau_{31}$ and $\tau'_{13}=\tau'_{31}$. The textbook discussions cited here [3,22–24] provide the background for the moment-balance construction. The additional step considered below is to require corresponding equalities about other axes of the same finite element. Whether those equalities refer to a common point is essential to assessing the argument.

The author then chooses BB' and DD' as alternative axes and imposes $\tau_{31}=\tau'_{13}$ and $\tau_{13}=\tau'_{31}$. Combining all four equalities gives $\tau_{13}=\tau_{31}=\tau'_{13}=\tau'_{31}=\tau$, as illustrated in Figure 2. Under these additional conditions, the selected shear components have no difference across the element. The author interprets this result as excluding the first-order increments shown in Figure 1. This conclusion is conditional on the imposed cross-position equalities; local tensor symmetry alone does not require them.

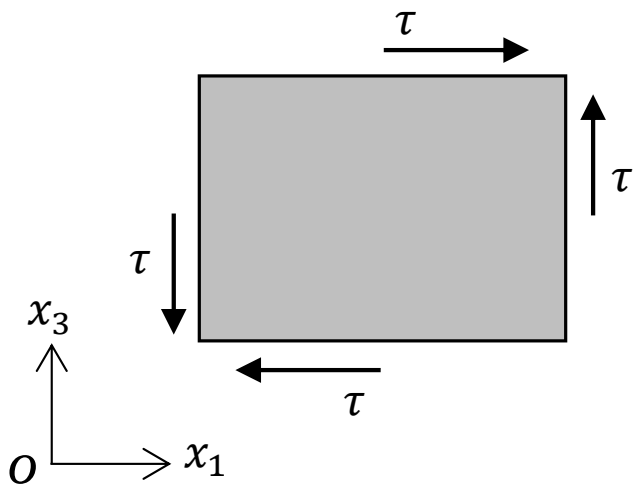


Figure 2. Equal Face Stresses Imposed in the Author's Construction

The preceding manuscript extends this equal-stress construction to the surrounding domain [21]. If the resulting field were spatially uniform, its stress divergence would vanish and it could not generate the viscous-force density in the momentum equation. The crucial issue is therefore the validity of the added equalities, rather than the consequence of differentiating a genuinely uniform field.

The author's proposed conclusion is that the imposed equal-stress construction eliminates viscous-force gradients. This should be read as a conclusion about that construction, not as an established proof that every symmetric stress tensor must be spatially uniform.

3.2. On the Conflicts Between Calculus and SST for Fluids

For a two-dimensional illustration, the element in Figure 3 is used to compare spatial increments of the two shear components. The first-order expressions are $\tau'_{13} = \tau_{13} + (\partial\tau_{13}/\partial x_3)\Delta x_3$ and $\tau'_{31} = \tau_{31} + (\partial\tau_{31}/\partial x_1)\Delta x_1$. The derivatives are taken in different directions, and the primed quantities generally refer to different positions on the element.

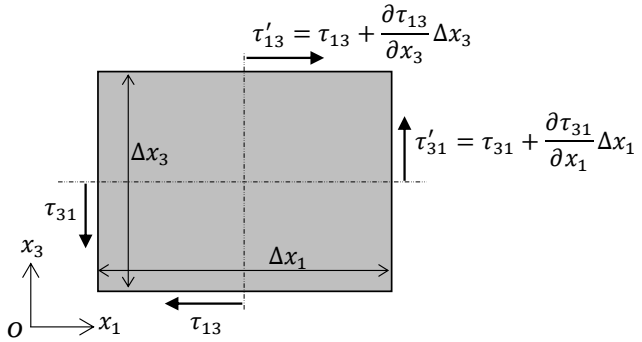


Figure 3. Fluid Element and Directional Shear-Stress Increments

Under the equalities imposed in the author's construction, the following relations are obtained:

$$\tau_{31} = \tau_{13}, \tag{7a}$$

$$\tau_{31} + \frac{\partial\tau_{31}}{\partial x_1}\Delta x_1 = \tau_{13} + \frac{\partial\tau_{13}}{\partial x_3}\Delta x_3. \tag{7b}$$

Combining Eqs. (7a) and (7b) gives the following relation between the selected increments:

$$\frac{\partial\tau_{13}}{\partial x_3} = \frac{\partial\tau_{31}}{\partial x_1}\left(\frac{\Delta x_1}{\Delta x_3}\right). \tag{8}$$

The relation in Eq. (8) connects $\partial\tau_{13}/\partial x_3$ and $\partial\tau_{31}/\partial x_1$ through the element ratio $\Delta x_1/\Delta x_3$. The author considers a sufficiently small element and asks what happens if Δx_1 is doubled while Δx_3 remains fixed. If one derivative is held unchanged, the imposed relation would require the other to change with the aspect ratio. This is interpreted as a dependence of the stress calculation on the selected element dimensions. The inference follows from the cross-position equality used to obtain Eq. (8); it is not a general consequence of equality between two tensor components at the same point.

The author notes that practical flow computations do not normally solve this imposed relation directly; they solve the momentum equations. Consequently, the proposed aspect-ratio argument does not, by itself, demonstrate a failure of grid convergence in a conventional discretization. A numerical convergence claim would require a specified scheme and a consistent refinement study.

The author's argument:

The planar Poiseuille-flow example makes the distinction between local component equality and directional spatial variation more explicit. The author uses this example to examine the compatibility of the particular primed-stress equalities with a nonzero pressure gradient.

Planar Poiseuille flow occurs between two stationary parallel plates and is driven by a streamwise pressure gradient, denoted here by $\Delta p/\Delta x$. For the steady, fully developed laminar configuration, the velocity profile is written as

$$u = -\frac{1}{2\mu}\left(\frac{\Delta p}{\Delta x}\right)(H - z)z; \quad w = 0. \tag{9}$$

The velocity profile in Figure 4 has a streamwise component that varies across the channel and no transverse velocity component.

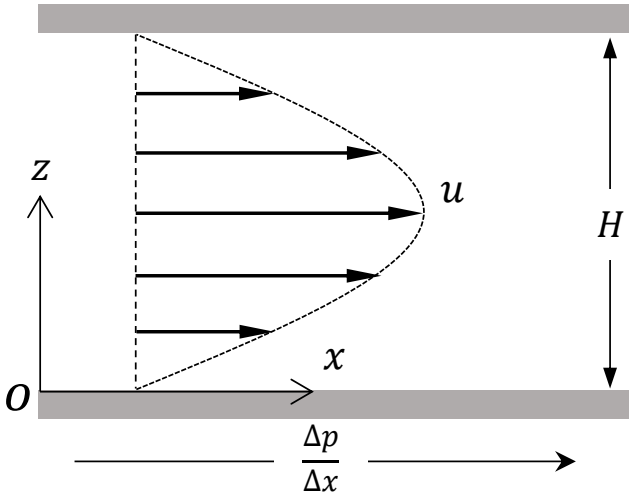


Figure 4. Planar Poiseuille Velocity Profile Under an Applied Pressure Gradient

Using the symmetric constitutive relation, the relevant stress components are

$$\tau_{xz} = \tau_{zx} = \mu\left(\frac{\partial u}{\partial z} + \frac{\partial w}{\partial x}\right) = \left(\frac{\Delta p}{\Delta x}\right)\left(z - \frac{H}{2}\right), \tag{10}$$

Their directional derivatives with respect to z and x, respectively, are

$$\frac{\partial \tau_{xz}}{\partial z} = \frac{\Delta p}{\Delta x}; \quad \frac{\partial \tau_{zx}}{\partial x} = 0. \tag{11}$$

Applying first-order spatial increments to the element in Figure 5 gives the stresses at the upper and right faces. The increments are Δz and Δx, respectively, although both dimensions are not shown explicitly in the illustration:

$$\begin{cases} \tau'_{zx} = \tau_{zx} + \dfrac{\partial \tau_{zx}}{\partial x}\Delta x = \tau_{zx} + \left(\dfrac{\Delta p}{\Delta x}\right)\Delta x, \\ \tau'_{xz} = \tau_{xz} + \dfrac{\partial \tau_{xz}}{\partial z}\Delta z = \tau_{xz}, \end{cases} \tag{12}$$

These expressions use the directional derivatives given in Eq. (11).

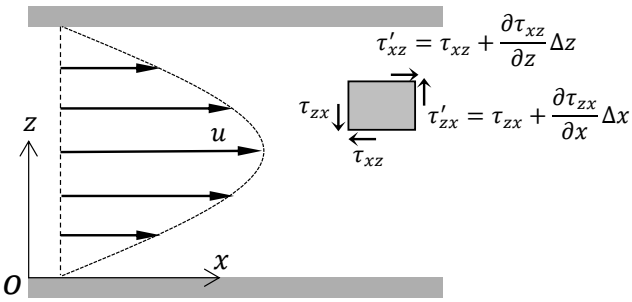


Figure 5. Planar Poiseuille Velocity Profile and Viscous-Stress Components

The author compares the primed components in Eq. (12) with the local equality $\tau_{zx} = \tau_{xz}$. Because the imposed pressure gradient is nonzero, the two selected increments do not produce equal primed values. The proposed objection is that symmetry cannot be retained under this construction. However, the primed stresses occupy different spatial positions: a symmetric tensor may vary with z while remaining independent of x. The

example therefore requires careful separation of local symmetry from the additional equality between different face locations.

The Poiseuille profile provides a direct way to organize the comparison without changing the prescribed velocity field. At a fixed point, the two symmetric shear components have the same value. Moving vertically changes that common value because the streamwise velocity gradient changes with height. Moving horizontally does not change it in a fully developed flow. These two statements are compatible: equality of functions does not require their derivatives with respect to different independent variables to be equal. The directional derivative must be taken with respect to the same coordinate before component equality is differentiated. Thus, the comparison between an upper face and a right face includes both a component selection and a position change. Separating those operations is essential to interpreting the primed quantities. This also explains why the same example cannot establish an unavoidable dependence on grid aspect ratio without first establishing the cross-position premise used to derive that dependence. The physical continuum solution is fixed before a numerical mesh is chosen, and the discretization is then evaluated according to how faithfully it approximates that solution.

3.3. On the Calculation of the Lift and Drag on Airfoils

The wall-force construction in Figure 6 illustrates the usual calculation of lift along the y axis and drag along the x axis. Under the appropriate local wall-coordinate and boundary conditions, the commonly used wall-shear expression is [3,5,6,23,25,26]

$$\tau = \mu \left(\frac{\partial u}{\partial y} \right)_{y=0}, \tag{13}$$

where τ is wall shear stress, measured in Pa or $\mathrm{N/m^2}$. The coordinate y is normal to the local wall, u is the tangential velocity component, and $y = 0$ denotes the wall surface. The derivative is evaluated at that surface.

The wall shear stress acts tangentially, while pressure contributes normally to the airfoil surface. Their projections onto directions perpendicular and parallel to the incoming flow define lift L and drag D, respectively. The corresponding expressions are written as [3,25]

$$\begin{cases} L = \displaystyle\int_{LE}^{TE} \left(-p_u \cos\theta + \tau_u \sin\theta \right) ds + \int_{LE}^{TE} \left(-p_l \cos\theta + \tau_l \sin\theta \right) ds, \\ D = \displaystyle\int_{LE}^{TE} \left(-p_u \sin\theta + \tau_u \cos\theta \right) ds + \int_{LE}^{TE} \left(-p_l \sin\theta + \tau_l \cos\theta \right) ds, \end{cases} \tag{14}$$

The integrals extend from the leading edge (LE) to the trailing edge (TE) on both surfaces. Subscripts u and l identify the upper and lower airfoil surfaces, respectively.

Such force calculations form part of established aerodynamic analysis. The broader role of computational fluid dynamics in aircraft design and its remaining challenges are discussed by Witherden and Jameson [27] and by Spalart and Venkatakrishnan [28]. These applications provide context for examining wall traction, but their success does not remove the need to state the tensor and surface-normal conventions consistently.

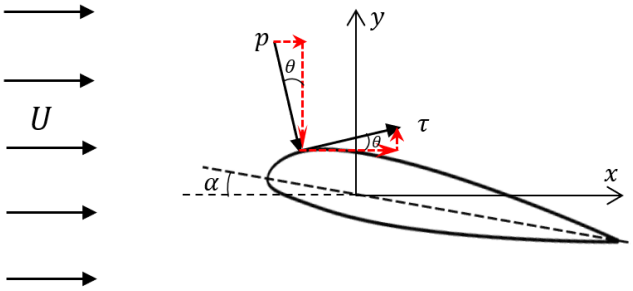


Figure 6. Pressure and Tangential Wall Stress on an Airfoil at Incidence

The author's argument:

The author argues that an additional component, denoted τ' and shown in red in Figure 7, should be included when a symmetric stress tensor is used. In this interpretation, τ' is perpendicular to the tangential stress τ and has the same magnitude. It is treated as acting opposite to the local pressure contribution. This is a proposed interpretation of the tensor components; the actual wall traction must be determined using the tensor contracted with the wall normal.

With that additional proposed wall component, the author's force decomposition gives the following alternative lift and drag expressions:

$$\begin{cases} L = \int_{LE}^{TE} [(\tau_u' - p_u)\cos\theta + \tau_u \sin\theta]\, ds + \int_{LE}^{TE} [(\tau_l' - p_l)\cos\theta + \tau_l \sin\theta]\, ds, \\ D = \int_{LE}^{TE} [(\tau_u' - p_u)\sin\theta + \tau_u \cos\theta]\, ds + \int_{LE}^{TE} [(\tau_l' - p_l)\sin\theta + \tau_l \cos\theta]\, ds. \end{cases} \tag{15}$$

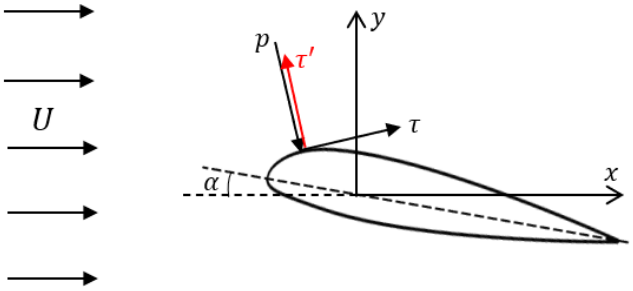


Figure 7. Additional Wall Component Proposed in the Author's SST Interpretation

The author is not aware of standard airfoil calculations using these additional terms. One possible approximation discussed in the source manuscript is that their magnitude could be small relative to the pressure contribution in attached flow. However, the more fundamental question is whether the proposed component belongs to the traction on that particular surface. A small contribution and an incorrectly assigned surface component are different issues and should not be conflated.

The author's argument requires both proposed components to enter the wall-force calculation whenever they are nonzero. In that interpretation, equal tangential and transverse components would modify the expressions in Eq. (14). The sphere example is then introduced because the viscous and pressure contributions are of comparable importance in creeping flow. The author finds an unchanged drag expression but a nonzero transverse result after adding the proposed component. This outcome motivates the following comparison. It does not independently establish an inconsistency in symmetric stress, because the physical force depends on the traction on the actual sphere surface and on the full three-dimensional surface integration.

A wall-force calculation should begin with the local unit normal and the complete traction vector. Under the index convention used in the Cartesian momentum balance, the normal contracts with the tensor's surface-normal index. The tangential wall force is then the tangential projection of that resulting vector. A complementary shear component refers to a different orientation of the imagined surface on which traction is being evaluated; it is not automatically a second independent force acting on the original wall. This geometric distinction is separate from Newton's third law, which relates the forces exerted across a common interface. Pressure and viscous traction can subsequently be projected into lift and drag directions and integrated over the body. For a curved wall, the local normal and tangent change along the surface, so the projection must be performed consistently at each location. These steps provide a common basis for assessing both the conventional and the proposed expressions. They also distinguish a legitimate boundary-layer simplification

of wall traction from an assertion that the tensor has silently changed from symmetric to nonsymmetric.

3.4. On Stokes' Drag Law

Stokes' drag law is a major analytical result in viscous-fluid mechanics. The historical work examined pendulum motion with fluid friction and provided the creeping-flow resistance of a sphere [29]. The sphere-drag relation subsequently became a basis for viscosity measurements, including falling-sphere viscometers [30]. Its scientific influence extends well beyond this single application.

Cartwright discusses the historical connections between Stokes' law, viscometry, and several Nobel-recognized developments [31]. Millikan's work used a correction to Stokes' law in determining electrical charge [32]. These examples illustrate the significance of the drag relation while remaining distinct from a proof of any particular interpretation of tensor components.

Stokes used a symmetric viscous-stress formulation in his development of fluid-motion equations [33]. The practical success of the drag law consequently supports the usefulness of that framework, although a single force result cannot uniquely identify every constitutive assumption. The following calculation reproduces the conventional sphere-flow expressions and then presents the author's proposed additional terms. The two calculations must be compared using a common definition of surface traction.

The conventional sphere-flow solution is summarized first, following Stokes and later treatments [29,34,35]. A sphere of radius a translates at speed U to the right, or equivalently remains stationary while the far-field flow approaches from the right, as shown in Figure 8. In the steady creeping-flow approximation, inertia is neglected and the momentum equation reduces to

$$\nabla p = \mu \nabla^2 \vec{V} \quad \& \quad \nabla \cdot \vec{V} = 0. \tag{16}$$

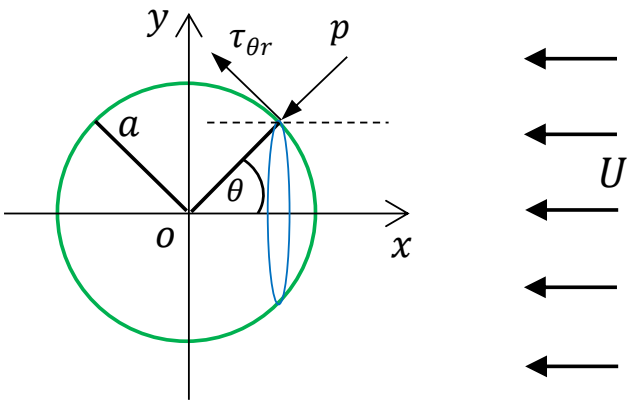


Figure 8. Pressure and Viscous Traction on the Sphere Surface

The flow is axisymmetric about the x axis. A spherical-coordinate description can therefore be expressed through the meridional variables r and θ shown in Figure 8. The boundary conditions are

$$\begin{cases} u_r = 0, \quad u_\theta = 0 \quad \text{when } r = a, \\ u_r = -U\cos\theta, \quad u_\theta = U\sin\theta \quad \text{when } r = \infty. \end{cases} \tag{17}$$

Here r is the radial distance from the sphere center, and θ is the angle measured from the x axis in the illustrated meridional plane. The indicated positive orientation fixes the component signs.

Solving the creeping-flow problem gives the following velocity components:

$$\begin{cases} u_r = -U\cos\theta\left(1 - \dfrac{3a}{2r} + \dfrac{a^3}{2r^3}\right), \\ u_\theta = U\sin\theta\left(1 - \dfrac{3a}{4r} - \dfrac{a^3}{4r^3}\right), \end{cases} \tag{18}$$

The corresponding pressure field is

$$p = \mu\cos\theta\,\frac{\partial}{\partial r}\left(\frac{\partial^2}{\partial r^2} - \frac{2}{r^2}\right)\left[\frac{1}{4}Ua^2\left(-\frac{2r^2}{a^2} + \frac{3r}{a} - \frac{a}{r}\right)\right] = \frac{3}{2}\mu U\frac{a}{r^2}\cos\theta. \tag{19}$$

On the sphere surface, these expressions become

$$p|_{r=a} = \frac{3\mu U}{2a}\cos\theta. \tag{20}$$

White and Majdalani [34] and Lautrup [36] present corresponding expressions with the opposite far-field flow direction. Signs must therefore be compared using the stated orientation.

For the symmetric constitutive relation, the shear components evaluated on the sphere surface take the form

$$\tau_{\theta r}^{sym}\Big|_{r=a} = \tau_{r\theta}^{sym}\Big|_{r=a} = \mu\left(\frac{1}{r}\frac{\partial u_r}{\partial\theta} + \frac{\partial u_\theta}{\partial r} - \frac{u_\theta}{r}\right)_{r=a} = \frac{3\mu U}{2a}\sin\theta. \tag{21}$$

Following the conventional treatment [29,34,36], the axial drag is obtained by integrating the relevant pressure and viscous-traction projections over the sphere surface shown in Figure 8:

$$D = -\int_S \tau_{\theta r}|_{r=a}\sin\theta\,dA - \int_S p|_{r=a}\cos\theta\,dA = -4\pi\mu Ua - 2\pi\mu Ua = -6\pi\mu Ua, \tag{22}$$

Here $dA = 2\pi a^2\sin\theta\,d\theta$ is the area of a spherical ring associated with the polar increment $d\theta$. The negative sign of D follows from the chosen flow direction; the drag magnitude is $6\pi\mu Ua$.

The author's argument:

Using the same pressure and shear expressions, the author writes the following transverse-force integral:

$$L = \int_S \tau_{\theta r}|_{r=a}\cos\theta\,dA - \int_S p|_{r=a}\sin\theta\,dA = 0. \tag{23}$$

The displayed calculation gives the familiar drag magnitude and a zero transverse result for the unmodified expression. Axisymmetry requires the net transverse force to vanish. When interpreting a transverse projection, the azimuthal cancellation over the complete sphere must be retained; the spherical-ring area alone is directly suited to an axisymmetric axial projection.

The author next introduces the additional component $\tau_{r\theta}$ shown in red in Figure 9, alongside $\tau_{\theta r}$. Their equality follows from symmetry at a common point, but assigning both to the same physical surface requires examination of the surface-normal index. The calculation below retains the author's proposed assignment for comparison.

Including this proposed additional component gives the following modified axial-force integral:

$$D = -\int_S \tau_{\theta r}|_{r=a}\sin\theta\,dA + \int_S (\tau_{r\theta} - p)|_{r=a}\cos\theta\,dA = -4\pi\mu Ua - 2\pi\mu Ua = -6\pi\mu Ua. \tag{24}$$

In the displayed calculation, the added term integrates to zero in the axial direction, leaving the conventional drag magnitude unchanged.

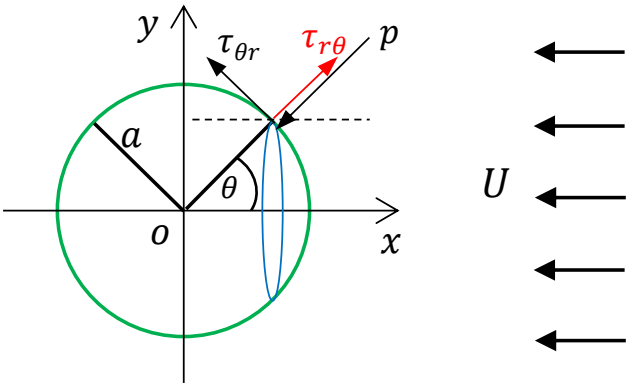


Figure 9. Additional Sphere-Surface Component Proposed in the SST Calculation

For the corresponding proposed transverse-force calculation, the author obtains

$$L = \int_S \tau_{\theta r}|_{r=a} \cos\theta \, dA + \int_S (\tau_{r\theta} - p)|_{r=a} \sin\theta \, dA = 4\pi\mu U a. \tag{25}$$

This expression gives a nonzero transverse quantity, which the author interprets as a contradiction with the axisymmetric flow. The result instead requires checking both the traction assignment and the azimuthal integration before it can be used to draw a conclusion about tensor symmetry. It is retained here as the contested calculation developed in the manuscript.

The geometry of the sphere adds a further distinction. An axisymmetric pressure or shear magnitude depends on the polar angle but not on azimuth. Its axial projection can therefore be integrated over a complete ring using the factor 2π. A transverse Cartesian projection includes an azimuthal directional factor, and the contributions around that ring cancel. A meridional component drawn on one side of a two-dimensional sketch is therefore not itself the net three-dimensional lift. The same consideration applies whether the constitutive tensor is symmetric or nonsymmetric: the geometry of the surface integration cannot be altered by renaming the stress components. The force comparison must use the same surface, normal orientation, and coordinate basis in both cases. If a modified expression gives a transverse result for an otherwise axisymmetric field, the first task is to inspect those projections and integration limits. Only after that check can the result be attributed to a constitutive difference. This distinction preserves the usefulness of the sphere as a test problem while avoiding a conclusion based solely on a meridional force sketch.

Section 6 presents the corresponding calculation using the proposed AST and compares its drag and transverse-force expressions with those given above.

3.5. On Stresses, Energy Transfer and Dissipation in the Rigid Rotating Flows

Rigid-body rotation can occur in fluid confined between two concentric cylinders of radii R_1 and R_2 when both cylinders rotate at the same angular velocity ω, as illustrated in Figure 10. After the transient motion has decayed, the fluid can rotate with the cylinders without a rate of deformation. This example is frequently used to distinguish rotation from strain in continuum mechanics. Under the conventional Newtonian relation, the viscous stresses vanish in exact rigid-body rotation. The total stress need not vanish, because pressure remains present and supplies the radial force required by the rotating motion. The discussion below concerns viscous stress and viscous stress power, not the absence of all forces in the fluid.

In two-dimensional polar coordinates, the velocity field for rigid-body rotation is written as

$$\begin{cases} u_\theta = \omega r, \\ u_r = 0, \end{cases} \tag{26}$$

where r is the distance from the rotation axis to the point under consideration. The conventional symmetric viscous-stress components are given by [37]

$$\begin{cases} \tau_{rr} = 2\mu \dfrac{\partial u_r}{\partial r}; \quad \tau_{\theta\theta} = 2\mu \left(\dfrac{1}{r} \dfrac{\partial u_\theta}{\partial \theta} + \dfrac{u_r}{r} \right), \\ \tau_{\theta r} = \tau_{r\theta} = \mu \left(\dfrac{1}{r} \dfrac{\partial u_r}{\partial \theta} + \dfrac{\partial u_\theta}{\partial r} - \dfrac{u_\theta}{r} \right), \end{cases} \tag{27}$$

Substitution of the rigid-rotation velocity field gives zero viscous stress because

$$\begin{cases} \tau_{rr} = 0; \quad \tau_{\theta\theta} = 0, \\ \tau_{\theta r} = \tau_{r\theta} = 0. \end{cases} \tag{28}$$

The conventional symmetric relation therefore gives zero viscous dissipation for this exact velocity field. This result follows from the vanishing rate of deformation, despite the nonzero velocity gradient. It does not assert that pressure vanishes or that every conceivable externally loaded rotating apparatus can preserve exact rigid-body motion. The example below introduces additional loading and asks whether viscous torque can be transferred while the same kinematics are retained.

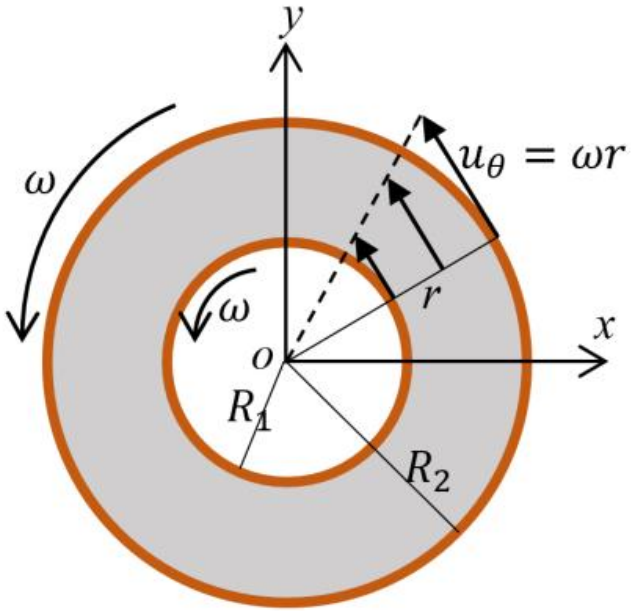


Figure 10. Concentric Cylinders and the Rigid-Body Rotation Configuration

The author's argument:

Consider the concentric-cylinder configuration in Figure 10. The outer cylinder is called the driving cylinder and the inner cylinder the following cylinder. They are mounted on separate shafts, with no solid mechanical connection between them; their interaction is through the intervening fluid. If both cylinders and the fluid rotate at angular speed ω, the resulting velocity field is that of rigid-body rotation. This description specifies the kinematics, but a sustained torque-transfer example also requires a compatible mechanical balance and constitutive relation.

In an idealized unloaded configuration with no resisting bearing torque, the cylinders and fluid can maintain their established rotation without a continuing driving torque. Zero viscous stress is compatible with this motion. The pressure field provides the radial acceleration, while the absence of a viscous torque means that no viscous power is transmitted

between the cylinders. This is the situation represented by the conventional rigid-rotation solution.

Now introduce a resisting torque on the inner cylinder and a compensating driving torque on the outer cylinder. The author assumes that the entire system nevertheless continues to rotate at the same angular speed. Under this assumption, input power must pass through the fluid to balance the resisting load. The question is whether that state is compatible with the material law. For a classical Newtonian fluid, transmitting a steady viscous torque requires deformation; exact common-speed rigid rotation does not supply that deformation. The proposed example therefore requires a justified constitutive mechanism or a departure from exact rigid-body rotation.

Denoting the resisting torque magnitude by T_{inner}, the associated dissipated power at angular speed ω is

$$P_{diss} = \omega T_{inner}, \tag{29}$$

The corresponding applied power at the outer cylinder is

$$P_{driving} = \omega T_{outer}, \tag{30}$$

where T_{outer} is the applied torque magnitude. If the source and load rotate at the same angular speed and no other losses are admitted, the assumed steady power balance requires $P_{driving} = P_{diss}$, giving

$$T_{outer} = T_{inner}. \tag{31}$$

The equality states that the applied torque balances the resisting torque under the specified assumptions. The author interprets this as requiring nonzero fluid shear stresses to transmit torque from the outer cylinder to the inner cylinder. That interpretation identifies a necessary stress for the proposed loaded state, but it does not establish that the state can remain an exact rigid-body rotation for an ordinary Newtonian fluid. The constitutive and kinematic conditions must also be mutually compatible.

The proposed counterexample therefore raises a constitutive question about loaded rotation. It does not establish that the symmetric Newtonian relation fails for its own exact rigid-rotation solution.

The cylinder example also requires a distinction between exact and approximate rigid rotation. With a sufficiently small resisting load, two cylinders can rotate at nearly the same speed while a small relative velocity gradient transmits viscous torque through the intervening fluid. Such a state may look close to rigid rotation in a schematic drawing, but the small deformation is precisely what supports the Newtonian viscous stress. Taking the deformation to zero while keeping a finite torque fixed is therefore not the same limiting process as letting both the deformation and transmitted torque tend to zero. The mechanical specification must state which quantities are controlled: the cylinder speeds, the applied torques, or some combination determined by the drive and load. Once those controls are specified, the velocity field follows from the governing equations and boundary conditions. Assuming common angular velocity and an independently prescribed finite transmitted viscous torque can overconstrain the classical model. The proposed AST must likewise be evaluated with compatible controls, rather than being assigned a torque-transfer role solely because its components remain nonzero for a rotating velocity field.

3.6. On Energy Dissipation in Compressible Flows

The conventional local viscous-dissipation expression is written as the contraction of viscous stress with the velocity gradient:

$$\Phi = \tau_{ij} \frac{\partial u_i}{\partial x_j}. \tag{32}$$

This expression has the dimensions of power per unit volume. Its physical interpretation depends on the constitutive relation and the energy balance in which it appears. The following discussion examines the compressible form; Section 8 returns to the alternative expression proposed for the AST.

Substituting the symmetric components from Eq. (3) and the stated second-viscosity relation gives

$$\Phi = \mu\left\{2\left[\left(\frac{\partial u}{\partial x}\right)^2+\left(\frac{\partial v}{\partial y}\right)^2+\left(\frac{\partial w}{\partial z}\right)^2\right]+\left(\frac{\partial u}{\partial y}+\frac{\partial v}{\partial x}\right)^2+\left(\frac{\partial w}{\partial y}+\frac{\partial v}{\partial z}\right)^2+\left(\frac{\partial u}{\partial z}+\frac{\partial w}{\partial x}\right)^2 -\frac{2}{3}\left(\frac{\partial u}{\partial x}+\frac{\partial v}{\partial y}+\frac{\partial w}{\partial z}\right)^2\right\}. \tag{33}$$

This expression appears in standard treatments [6,34]. The negative final term follows from Stokes' hypothesis, $\lambda = -2\mu/3$. For incompressible flow, the velocity divergence vanishes and this term is zero. The remaining squared terms give a nonnegative dissipation rate, which may be zero when the deformation rate is zero. The irreversible conversion is from mechanical energy to internal energy; the expression does not imply destruction of total energy.

For compressible flow under the same hypothesis, rearranging the normal-gradient terms gives the equivalent expression

$$\Phi = \mu\left\{\frac{2}{3}\left[\left(\frac{\partial u}{\partial x}-\frac{\partial v}{\partial y}\right)^2+\left(\frac{\partial v}{\partial y}-\frac{\partial w}{\partial z}\right)^2+\left(\frac{\partial u}{\partial x}-\frac{\partial w}{\partial z}\right)^2\right]+\left(\frac{\partial u}{\partial y}+\frac{\partial v}{\partial x}\right)^2 +\left(\frac{\partial w}{\partial y}+\frac{\partial v}{\partial z}\right)^2+\left(\frac{\partial u}{\partial z}+\frac{\partial w}{\partial x}\right)^2\right\}. \tag{34}$$

This rearrangement also makes nonnegativity explicit. Studies of high-speed flow describe important processes of energy conversion, transfer, and heating [38,39]. However, those observations do not establish a universal rule that every nonzero velocity divergence must increase viscous dissipation relative to an unspecified incompressible comparison. The source manuscript used AI-generated explanations as part of this discussion; those explanations are not retained as scientific evidence. The relevant mechanisms instead require separate physical definitions and appropriate literature support.

Four mechanisms must be distinguished. First, shocks involve irreversible changes and require a consistent thermodynamic description. Second, viscous dissipation depends on deformation rates and constitutive coefficients, rather than on compressibility alone. Third, compressible turbulence contains pressure–velocity and density correlations that affect energy redistribution and must be treated within the relevant averaged or resolved equations. Fourth, acoustic radiation transports energy away from a region, whereas its eventual absorption converts that energy into heat. These processes can coexist in high-speed systems, but their contributions cannot be inferred solely from the sign of one term in a local viscous-stress formula.

The following example examines a particular dilatational velocity field under Stokes' hypothesis and identifies the precise condition under which the conventional viscous-dissipation expression vanishes.

The author's argument:

Although Eq. (34) is nonnegative, it need not be strictly positive for every compressible velocity field. Consider the special case defined by

$$\frac{\partial u}{\partial x}=\frac{\partial v}{\partial y}=\frac{\partial w}{\partial z}=\varepsilon\neq 0 \quad \text{and} \quad \frac{\partial u_i}{\partial x_j}=0 \quad \text{for } i\neq j. \tag{35}$$

The velocity divergence is nonzero for this field, since

$$\nabla \cdot \vec{V} = \frac{\partial u}{\partial x} + \frac{\partial v}{\partial y} + \frac{\partial w}{\partial z} = 3\varepsilon \neq 0. \tag{36}$$

Substitution into the stated dissipation expression gives

$$\Phi = 0. \tag{37}$$

The displayed zero results from isotropic dilation under the zero-bulk-viscosity implication of Stokes' hypothesis. The author originally interprets it as a contradiction with increased dissipation in compressible flow. That interpretation requires qualification: a negative second viscosity coefficient does not imply negative bulk viscosity, and a zero result for this idealized field does not violate nonnegative dissipation. A nonzero bulk viscosity changes the dilatational contribution without requiring a nonsymmetric Cauchy stress.

The distinction between second viscosity and bulk viscosity is central to the compressible example. In the conventional three-dimensional isotropic Newtonian relation, bulk viscosity combines the second coefficient with two thirds of the shear viscosity. Stokes' hypothesis sets that combination to zero; it does not assert that every compressible process is reversible or that shocks cannot generate entropy. The isotropic dilatational velocity field used here has no deviatoric deformation, so its viscous dissipation depends on the bulk contribution. Other compressible fields can have substantial deviatoric deformation and positive shear-viscous dissipation even under the same hypothesis. Thermal conduction and other irreversible processes are also distinct contributions to entropy production. Consequently, the interpretation of Eq. (37) must be limited to the displayed constitutive model and velocity field. Comparing that result with a high-speed flow containing shocks, temperature gradients, and turbulence requires additional information rather than an appeal to compressibility alone. This coefficient distinction also prevents the positive value chosen for the AST momentum equation from being mistaken for a direct measurement of the conventional bulk viscosity.

4. AST for Fluids and the Derivation of the N–S Equation

The preceding section presents the author's objections and identifies assumptions that require particular care. This section introduces the proposed AST and examines the momentum equation obtained from it. The proposal differs from the conventional symmetric Newtonian relation by retaining individual velocity-gradient components rather than their symmetric combinations. The author motivates this choice by reference to simple-shear viscosity. Extending a simple-shear law to arbitrary three-dimensional motion is nevertheless a constitutive choice, and the resulting relation must be checked against angular-momentum balance, observer invariance, and the energy equation.

4.1. Asymmetric Stress Tensor (AST) for Fluids

Sheng [18] previously proposed this asymmetric relation for fluid viscous stresses. Its components resemble the simple-shear expression associated with Newton's law of viscosity. The present comparison uses the tensor notation of standard fluid-mechanics treatments [5,40], while keeping the proposed constitutive assumption explicit. The component expressions are

$$\left.\begin{aligned}
&\tau_{11} = \mu\left(\frac{\partial u_1}{\partial x_1}\right);\ \tau_{22} = \mu\left(\frac{\partial u_2}{\partial x_2}\right);\ \tau_{33} = \mu\left(\frac{\partial u_3}{\partial x_3}\right) \quad \text{- normal stresses}\\
&\tau_{12} = \mu\left(\frac{\partial u_1}{\partial x_2}\right);\ \tau_{21} = \mu\left(\frac{\partial u_2}{\partial x_1}\right) \quad \text{- asymmetric shear stresses}\\
&\tau_{13} = \mu\left(\frac{\partial u_1}{\partial x_3}\right);\ \tau_{31} = \mu\left(\frac{\partial u_3}{\partial x_1}\right) \quad \text{- asymmetric shear stresses}\\
&\tau_{23} = \mu\left(\frac{\partial u_2}{\partial x_3}\right);\ \tau_{32} = \mu\left(\frac{\partial u_3}{\partial x_2}\right) \quad \text{- asymmetric shear stresses}
\end{aligned}\right\} \tag{38}$$

Three differences from the SST are apparent. First, the displayed normal components lack the factor of two present in Eq. (3); the author discusses this factor in the preceding manuscript [21]. Second, each AST component contains a single velocity-gradient component. Third, a nonsymmetric second-order tensor has nine component slots in three dimensions, compared with six for a symmetric tensor. This component count does not establish that the nine velocity gradients are independently specifiable in a given flow, nor does it establish the physical superiority of either relation.

The earlier proposal [18] shows how the AST can reproduce a familiar viscous term in the Cartesian momentum equation under stated assumptions. The preceding manuscript [21] extends the associated objections to stress increments, wall shear, force integration, and energy transfer. The following sections revisit those examples using the proposed relation. Recovering the same divergence in a selected flow is an important algebraic observation, but it does not by itself establish equivalence of the tensors: boundary tractions, torques, and stress power can differ even when a bulk momentum equation has the same form.

Before examining the momentum equation, the author considers the response of fluid and solid elements to shear. The intended distinction is between elastic deformation and continuing fluid deformation. This distinction concerns material response; it does not remove the requirement to satisfy angular-momentum balance for either material.

4.2. What Happens When the AST Is Applied to Fluids?

In classical continua without couple stresses or body couples, stress symmetry follows from local angular-momentum balance. It is not restricted to solids and is not merely an assumption that a fluid particle behaves as a rigid body. The author's comparison below contrasts elastic and viscous response to an applied shear. Such a contrast can clarify the different deformation histories, but a proposed nonsymmetric fluid stress additionally requires the corresponding angular-momentum mechanism to be specified.

Suppose a shear stress τ_{13} is applied to the upper face of the solid element in Figure 11. The element deforms according to its elastic constitutive response, while its complete traction field must satisfy the appropriate force and moment balances. The author uses the equality $\tau_{13} = \tau_{31}$ to discuss the complementary shear components. This equality should be understood locally and should not be interpreted as a separate rule by which an arbitrary applied stress automatically creates an independent balancing surface force. The material deformation law and the angular-momentum balance play different roles in this description.

For a fluid element, the same applied shear produces continuing deformation rather than a fixed elastic strain. Figure 12(a) shows the applied component τ_{13}, and Figure 12(b) illustrates the resulting deformation. The author interprets the response through the simple-shear viscosity relation. In this example, the distinction between velocity and velocity gradient is important: a shear stress is related to deformation rate, not directly to a velocity component. The proposed scalar relation is written as

$$\tau_{13} = \mu\frac{\partial u_1}{\partial x_3}. \tag{39}$$

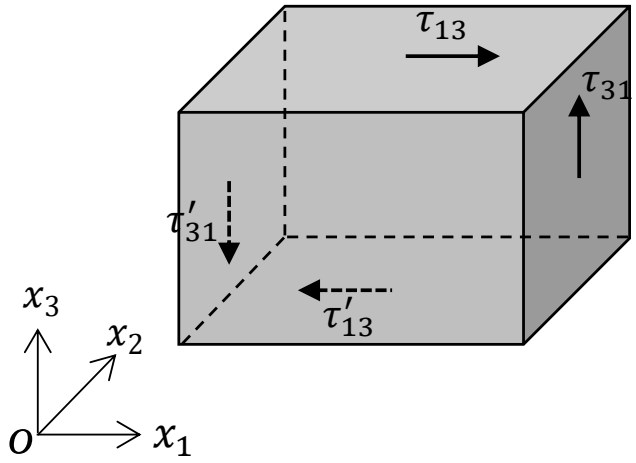


Figure 11. Applied Shear Stress on a Solid Element

The author interprets the applied shear as being balanced by the viscous response associated with the developing flow. The resulting simple-shear motion is the physical example represented in Figure 12. This interpretation concerns one loading configuration and does not, without a tensor constitutive argument, determine the other components for an arbitrary flow.

The source argument further assumes that a complementary component τ_{31} would require a separate vertical flow. That inference is not generally valid for a Newtonian constitutive relation. A nonzero stress component can arise from a cross derivative of another velocity component, and a nonzero component does not require a velocity in its own direction. The distinction is particularly clear in simple shear, where a symmetric stress tensor is compatible with a unidirectional velocity field.

An applied shear can therefore produce continuing fluid deformation. The existence and direction of that deformation do not alone decide whether the complete stress tensor is symmetric.

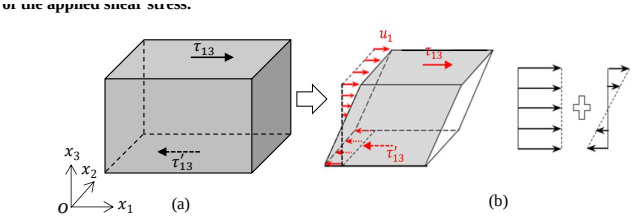


Figure 12. Applied Shear Stress and Deformation of a Fluid Element

4.3. Derivation of the N–S Equation with the AST

Substituting the proposed AST from Eq. (38) into the viscous-force density in Eq. (4), for constant μ, gives the following x-direction expression:

$$f_1^{vis} = \mu\left(\frac{\partial^2 u_1}{\partial x_1 \partial x_1} + \frac{\partial^2 u_1}{\partial x_2 \partial x_2} + \frac{\partial^2 u_1}{\partial x_3 \partial x_3}\right) = \mu\left(\frac{\partial^2 u_1}{\partial x_j \partial x_j}\right). \tag{40}$$

The displayed AST contribution to f_1^{vis} contains derivatives of u_1 alone. Its analogous components contain the corresponding velocity components. Any velocity-divergence contribution associated with the separate second-viscosity term must still be included when the complete viscous tensor is used.

Using the complete viscous tensor together with the proposed AST gives the momentum equation

$$\begin{cases} \rho\left(\dfrac{\partial u_1}{\partial t}+u_1\dfrac{\partial u_1}{\partial x_1}+u_2\dfrac{\partial u_1}{\partial x_2}+u_3\dfrac{\partial u_1}{\partial x_3}\right)=-\dfrac{\partial p}{\partial x_1}+f_{b1}+\mu\left(\dfrac{\partial^2 u_1}{\partial x_1\partial x_1}+\dfrac{\partial^2 u_1}{\partial x_2\partial x_2}+\dfrac{\partial^2 u_1}{\partial x_3\partial x_3}\right)+\lambda\dfrac{\partial(\nabla\cdot\vec{V})}{\partial x_1}, \\ \rho\left(\dfrac{\partial u_2}{\partial t}+u_1\dfrac{\partial u_2}{\partial x_1}+u_2\dfrac{\partial u_2}{\partial x_2}+u_3\dfrac{\partial u_2}{\partial x_3}\right)=-\dfrac{\partial p}{\partial x_2}+f_{b2}+\mu\left(\dfrac{\partial^2 u_2}{\partial x_1\partial x_1}+\dfrac{\partial^2 u_2}{\partial x_2\partial x_2}+\dfrac{\partial^2 u_2}{\partial x_3\partial x_3}\right)+\lambda\dfrac{\partial(\nabla\cdot\vec{V})}{\partial x_2}, \\ \rho\left(\dfrac{\partial u_3}{\partial t}+u_1\dfrac{\partial u_3}{\partial x_1}+u_2\dfrac{\partial u_3}{\partial x_2}+u_3\dfrac{\partial u_3}{\partial x_3}\right)=-\dfrac{\partial p}{\partial x_3}+f_{b3}+\mu\left(\dfrac{\partial^2 u_3}{\partial x_1\partial x_1}+\dfrac{\partial^2 u_3}{\partial x_2\partial x_2}+\dfrac{\partial^2 u_3}{\partial x_3\partial x_3}\right)+\lambda\dfrac{\partial(\nabla\cdot\vec{V})}{\partial x_3}. \end{cases} \tag{41}$$

The final terms in Eq. (41) arise from the separately specified volumetric contribution. Matching the coefficient in the conventional momentum equation, Eq. (5), requires the following value within this alternative constitutive representation:

$$\lambda=\frac{1}{3}\mu. \tag{42}$$

The positive coefficient obtained here differs from the value used with the symmetric representation under Stokes' hypothesis. Its sign cannot be compared in isolation from the tensor definition in which it appears. Section 8 examines the proposed energy expression, where thermodynamic admissibility requires consideration of the complete stress power.

Matching momentum equations is a useful consistency check, but its scope is limited. Two stress fields can have the same divergence over a selected domain while differing by a divergence-free tensor field. Their local force densities then agree, although their surface tractions and torques need not agree on every boundary. Their mechanical-power expressions can also differ because the velocity gradient contracts with the full stress, not merely its divergence. For that reason, reproducing Eq. (5) is not sufficient to identify the constitutive tensor uniquely. A stronger comparison would prescribe the same physical boundary data and test the force, moment, and energy consequences together. The viscosity coefficients must also be defined within their respective tensor relations before numerical values are compared. The present manuscript does not supply a new independent measurement that selects between the two descriptions. Its calculations should therefore be read as consequences of the stated proposed relation, with the additional balance and invariance conditions remaining part of the assessment.

5. The Proposed AST Resolution of the Conflicts

This section revisits the author's proposed resolutions using the AST. The calculations distinguish the local component relations from additional assumptions about different positions on a fluid element. The ability to write a nonsymmetric relation does not itself establish that symmetry caused the earlier difficulties.

5.1. On the Derivation of N–S Equation

The AST components are given in Eq. (38). Under this constitutive proposal, τ_{13} and τ_{31} need not be equal. Their values are determined by different velocity-gradient components, subject to the kinematic and boundary conditions of the chosen flow.

For the element in Figure 1, the first-order increments are $\tau'_{13}=\tau_{13}+(\partial\tau_{13}/\partial x_3)\Delta x_3$ and $\tau'_{31}=\tau_{31}+(\partial\tau_{31}/\partial x_1)\Delta x_1$. The AST does not impose equality between these two components, so no additional cross-component constraint is introduced by this constitutive choice. The author interprets the resulting nonuniform field as allowing the viscous-force divergence and hence the momentum equation to be derived. The differentiation itself is valid for any sufficiently smooth stress field, including a symmetric field whose components vary spatially. Thus, the contrast concerns the additional equality imposed in the earlier construction, rather than the applicability of calculus to symmetric tensors.

The stress increments shown in Figure 1 approach their corresponding directional derivatives as the element dimensions decrease. For a fixed smooth continuum field, those derivatives are determined by the field and are independent of the dimensions selected for a schematic element. This statement applies to the proposed AST expressions but does

not constitute a numerical convergence proof. A discrete solver can still have truncation error, mesh distortion, or insufficient resolution. Demonstrating grid convergence requires a specified discretization and systematic refinement while controlling the physical problem and boundary conditions. Removing the imposed relation between Δx_1 and Δx_3 avoids that particular artificial constraint, but no constitutive relation alone guarantees convergence of every numerical scheme.

5.2. On the Conflict of Calculus and SST in the Planar Poiseuille Flow

For planar Poiseuille flow, the proposed AST gives the following shear components:

$$\begin{cases} \tau_{xz} = \mu \dfrac{\partial u}{\partial z} = \left(\dfrac{\Delta p}{\Delta x}\right)\left(z - \dfrac{1}{2}H\right), \\ \tau_{zx} = \mu \dfrac{\partial w}{\partial x} = 0. \end{cases} \tag{43}$$

The unidirectional velocity profile gives a nonzero τ_{xz} under the proposed relation and a zero τ_{zx} because the transverse velocity vanishes. This result follows from the particular AST definition. It should not be generalized into a rule that every nonzero shear component requires a velocity in the same direction. Applying the spatial increments to the element in Figure 5 gives

$$\begin{cases} \tau'_{xz} = \tau_{xz} + \dfrac{\partial \tau_{xz}}{\partial z}\Delta z = \tau_{xz} + \left(\dfrac{\Delta p}{\Delta x}\right)\Delta z, \\ \tau'_{zx} = \tau_{zx} + \dfrac{\partial \tau_{zx}}{\partial x}\Delta x = \tau_{zx}. \end{cases} \tag{44}$$

Although Eq. (44) has the same incremental structure as Eq. (12), the component values now follow from the AST. The horizontal stress changes with Δz, while the zero component τ_{zx} has no streamwise increment. The author interprets this as avoiding the earlier primed-component equality. The underlying distinction remains between the selected constitutive relation and the additional spatial constraint used in the original objection.

6. Stokes' Flow: The Application of the AST

Section 3 presents the author's modified sphere-force calculation and its nonzero transverse result. This section retains the same comparison using the proposed AST. The result must be interpreted with the traction and spherical-integration qualifications already stated, rather than as an independent demonstration that a symmetric stress tensor predicts physical lift in an axisymmetric creeping flow.

The proposed AST components in the coordinate convention developed in the appendix are

$$\vec{\tau}^{asym}\Big|_{r=a} = \begin{bmatrix} \mu\left(\dfrac{\partial u_r}{\partial r}\right) & \mu\left(\dfrac{1}{r}\dfrac{\partial u_r}{\partial \theta} - \dfrac{u_\theta}{r}\right) \\ \mu\left(\dfrac{\partial u_\theta}{\partial r}\right) & \mu\left(\dfrac{1}{r}\dfrac{\partial u_\theta}{\partial \theta} + \dfrac{u_r}{r}\right) \end{bmatrix}_{r=a} = \begin{bmatrix} 0 & 0 \\ \dfrac{3\mu U}{2a}\sin\theta & 0 \end{bmatrix}. \tag{45}$$

At the sphere surface, the displayed AST gives $\tau_{\theta r}^{asym} = 3\mu U \sin\theta/(2a)$ and $\tau_{r\theta}^{asym} = 0$. The corresponding illustration is Figure 13. These values differ from the symmetric component pair in Eq. (21). The subsequent comparison shows how this difference enters the author's force expressions; it does not dispense with the need to identify which tensor component contributes to traction on the radial surface.

Using the stated force convention, the author's AST calculation of axial drag is

$$\begin{aligned} D &= \int_0^\pi \tau_{\theta r}^{asym}\Big|_{r=a} \sin\theta(2\pi a^2 \sin\theta\, d\theta) + \int_0^\pi (\tau_{r\theta}^{asym} - p)\Big|_{r=a} \cos\theta(2\pi a^2 \sin\theta\, d\theta) \\ &= -4\pi\mu U a - 2\pi\mu U a = -6\pi\mu U a. \end{aligned} \tag{46}$$

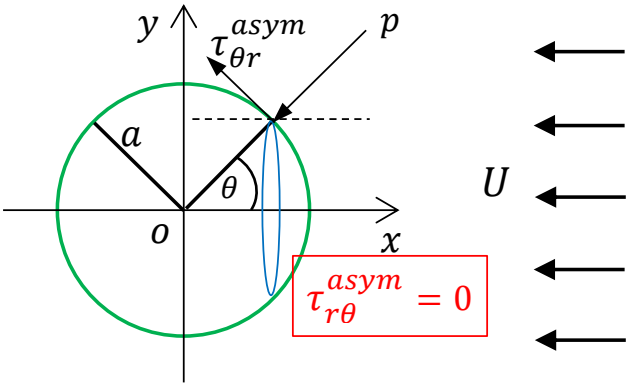


Figure 13. Pressure and Proposed AST Components on the Sphere Surface

The resulting drag magnitude agrees with Stokes' drag law. This agreement establishes the value of the displayed integral for this flow, while the broader physical equivalence of the constitutive descriptions requires separate checks of their tractions, torques, and energy balances.

The corresponding transverse expression under the author's AST calculation is

$$L = \int_0^{\pi} \tau_{\theta r}^{asym}\Big|_{r=a} \cos\theta(2\pi a^2 \sin\theta\, d\theta) + \int_0^{\pi} (\tau_{r\theta}^{asym} - p)\Big|_{r=a} \sin\theta(2\pi a^2 \sin\theta\, d\theta) = 0. \quad (47)$$

The displayed result is zero, as required for the net transverse force by axisymmetry. The full three-dimensional traction integral remains the appropriate reference for comparing force calculations.

7. Energy Transfer and Dissipation in Flows

Stress power provides an additional test of a constitutive proposal because the momentum equation alone does not determine how mechanical energy is transferred or converted. Rigid-body rotation is particularly useful: the conventional symmetric Newtonian tensor gives zero viscous stress, while the proposed AST can remain nonzero. As discussed in the cylinder example, this difference must be interpreted with compatible boundary loading and angular-momentum balance. The term stress-free in this discussion refers only to the viscous contribution, not to the pressure field [26].

The following analysis compares two kinematic configurations: planar Poiseuille flow, in which neighboring material positions can change their separation, and rigid-body rotation, which preserves the distance between material points. The source manuscript calls these sliding and nonsliding flows. These descriptions help explain the examples, but the constitutive and thermodynamic interpretation of stress power requires a local rate-of-deformation tensor and the relevant energy balance.

7.1. Energy Conservation Laws for Flows

7.1.1. Mechanical Energy in Fluid Motion

A mechanical-energy equation follows by multiplying the incompressible momentum equation, Eq. (6), by u_i and summing over the repeated velocity index. The resulting identity expresses the material rate of change of kinetic energy in terms of pressure, body-force, and viscous-force power:

$$\rho\left[\frac{\partial}{\partial t}\left(\frac{1}{2}u_i^2\right) + u_j\frac{\partial}{\partial x_j}\left(\frac{1}{2}u_i^2\right)\right] = -u_i\frac{\partial p}{\partial x_i} + u_i f_{bi} + u_i\frac{\partial \tau_{ij}}{\partial x_j}. \quad (48)$$

Here $u_i u_i/2$ is kinetic energy per unit mass, with summation over i. The left-hand side of Eq. (48) contains its material time derivative multiplied by density. The right-hand side contains the power contributions of the pressure gradient, body-force density, and

viscous-force density. This is a mechanical-energy identity and should be distinguished from an equation that also evolves internal energy.

The local viscous-force power $u_i \partial \tau_{ij} / \partial x_j$ can be positive or negative. A positive value represents a local contribution to kinetic energy, while a negative value represents a local removal. This term is not identical to the nonnegative viscous-dissipation function: the stress-work flux must also be considered. The internal-energy equation describes the conversion associated with dissipation and its relation to heating. Keeping the force-power, flux, and conversion terms distinct avoids interpreting a local negative kinetic-energy contribution as destruction of total energy.

7.1.2. Work Done by Fluid Viscous Stresses

Following the standard stress-work treatment [25], the divergence of the viscous stress-power flux is written as

$$W^{vis} = \frac{\partial (u_i \tau_{ij})}{\partial x_j}. \tag{49}$$

The velocity component u_i is contracted with the stress component carrying the same force-direction index. The resulting flux divergence has units of power per unit volume.

Applying the product rule separates this expression into

$$W^{vis} = u_i \frac{\partial \tau_{ij}}{\partial x_j} + \tau_{ij} \frac{\partial u_i}{\partial x_j}. \tag{50}$$

The first term on the right-hand side of Eq. (50) is the viscous-force power discussed above. The second is the contraction of stress with the velocity gradient. For the conventional Newtonian constitutive description, this contraction gives the viscous-dissipation function under the stated conditions [5,22,41]:

$$\Phi = \tau_{ij} \frac{\partial u_i}{\partial x_j}. \tag{51}$$

This contraction represents conversion from mechanical energy to internal energy for the conventional viscous model. The full velocity gradient contains both deformation and rotation, but a symmetric stress has zero contraction with the antisymmetric rotational part. The physical interpretation therefore concerns deformation rather than every nonzero spatial gradient of velocity.

Substitution of the symmetric relation and the stated volumetric coefficient gives the following expanded expression:

$$\begin{aligned} \Phi = \mu \Bigg\{ 2 \left[\left(\frac{\partial u}{\partial x} \right)^2 + \left(\frac{\partial v}{\partial y} \right)^2 + \left(\frac{\partial w}{\partial z} \right)^2 \right] + \left(\frac{\partial u}{\partial y} + \frac{\partial v}{\partial x} \right)^2 + \left(\frac{\partial w}{\partial y} + \frac{\partial v}{\partial z} \right)^2 \\ + \left(\frac{\partial u}{\partial z} + \frac{\partial w}{\partial x} \right)^2 - \frac{2}{3} \left(\frac{\partial u}{\partial x} + \frac{\partial v}{\partial y} + \frac{\partial w}{\partial z} \right)^2 \Bigg\}. \end{aligned} \tag{52}$$

The expression is given in standard treatments [41]. Its negative final term follows from Stokes' hypothesis, but the complete quadratic form is nonnegative. The isolated sign of a term in one algebraic representation does not determine the sign of total dissipation. This distinction becomes important when alternative coefficient definitions are compared.

The separation between stress-work transport and dissipation is particularly useful when interpreting a local negative or positive term. The divergence of a stress-power flux measures the net mechanical power passing into or out of a small region through its boundary. The stress contraction measures a local conversion term once the constitutive and energy equations have been specified. These quantities can have different signs and different spatial distributions even in a steady flow. Integrating the flux divergence over a

control volume converts it into a surface integral, whereas integrating a local conversion rate gives the total conversion within that volume. An algebraic rearrangement can move terms between displayed expressions, but it cannot remove the need for the same total balance. The distinction also fixes dimensions: multiplying stress by a velocity gradient gives power per volume, integrating over volume gives power, and integrating that power over time gives energy. The symbols used in the source equations are retained, but their physical interpretation must follow these units rather than the letter chosen to denote them.

7.1.3. The Total-Energy Equation for Fluid Motion

The manuscript writes the total-energy balance in the following form, following the cited treatments [5,22]:

$$\rho\left[\frac{\partial}{\partial t}\left(e+\frac{1}{2}u_i^2\right)+u_j\frac{\partial}{\partial x_j}\left(e+\frac{1}{2}u_i^2\right)\right]=\rho\dot{q}+\kappa\frac{\partial^2 T}{\partial x_k\partial x_k}+u_i f_{bi}-u_i\frac{\partial p}{\partial x_i}+u_i\frac{\partial \tau_{ij}}{\partial x_j}+\tau_{ij}\frac{\partial u_i}{\partial x_j}, \tag{53}$$

Here e denotes internal energy per unit mass. The displayed heat terms represent the specified volumetric heat input and conductive contribution, while the mechanical terms describe pressure work and viscous effects. A term labeled as dissipation converts mechanical energy to internal energy rather than adding energy from outside the system. The complete balance, including boundary heat and work fluxes, is needed to determine whether the local temperature rises.

7.2. Energy Transfer and Dissipation: In the Sliding Planar Poiseuille Flow

The material-element illustration in Figure 14 considers two small elements, e_1 and e_2, at different transverse positions in planar Poiseuille flow. Their positions at $t = t_1$ are shown in panel (a), and their downstream positions at $t = t_2$ in panel (b). Because the streamwise velocity varies with the transverse coordinate z, the elements can travel different streamwise distances over the same time interval. The particular illustrated ordering assumes that e_2 lies where the streamwise speed is greater. Deformation within each small element is omitted from this schematic comparison.

Comparing the element positions at the two times shows that their separation can change. The source manuscript calls this relative motion sliding. The example illustrates deformation in a sheared flow and provides a setting in which stress power and viscous dissipation can be evaluated explicitly. The relevant quantities are computed over a specified control volume rather than inferred solely from the visual displacement of the two elements.

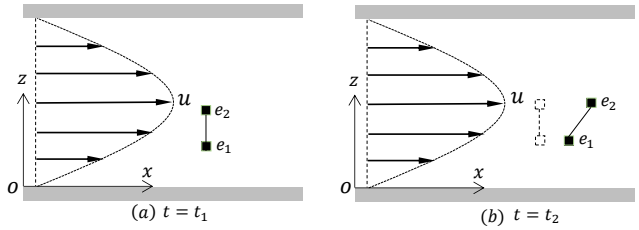


Figure 14. Relative Motion of Material Elements in Planar Poiseuille Flow

For the planar Poiseuille velocity profile, Eq. (51) gives the local dissipation rate

$$\Phi=\frac{1}{\mu}\left(\frac{\Delta p}{\Delta x}\right)^2\left(z-\frac{H}{2}\right)^2, \tag{54}$$

Integrating over the control volume outlined by the broken red lines in Figure 15 gives the dissipation rate per unit span:

$$E_\Phi = \int_0^{\Delta x}\int_0^{H} \frac{1}{\mu}\left(\frac{\Delta p}{\Delta x}\right)^2\left(z-\frac{H}{2}\right)^2 dx\,dz$$
$$= \frac{\Delta x}{\mu}\left(\frac{\Delta p}{\Delta x}\right)^2 \int_0^{H}\left(z-\frac{H}{2}\right)^2 dz = \frac{\Delta x}{12\mu}\left(\frac{\Delta p}{\Delta x}\right)^2 H^3. \tag{55}$$

The control volume has unit width in the y direction, which is not shown, height H, and streamwise length Δx. The imposed pressure difference over this length is Δp. Because a power density is integrated over volume, the quantity denoted E_Φ is a rate of energy conversion, not an accumulated energy.

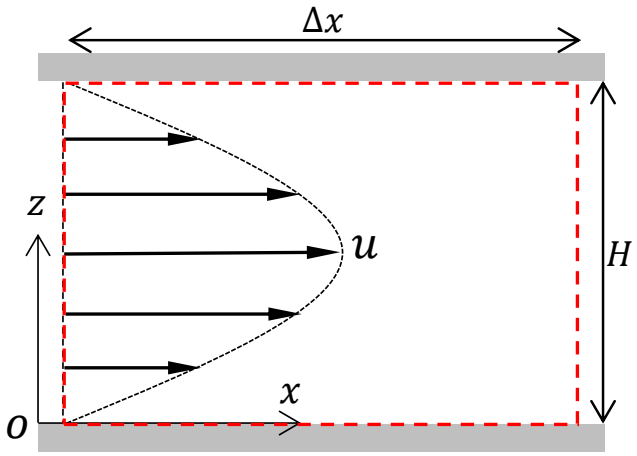


Figure 15. Control Volume for the Planar Poiseuille Power Balance

The pressure-gradient contribution to mechanical power is obtained by integrating the corresponding term in Eq. (48) over the same control volume:

$$E_{in} = \int_0^{H}\int_0^{\Delta x} -u\left(\frac{\partial p}{\partial x}\right) dx\,dz = -\Delta x \int_0^{H} u\left(\frac{\Delta p}{\Delta x}\right) dz = \frac{\Delta x}{12\mu}\left(\frac{\Delta p}{\Delta x}\right)^2 H^3. \tag{56}$$

The pressure gradient $\partial p/\partial x = \Delta p/\Delta x$ is constant. Integrating the viscous-force-power term of Eq. (48) gives

$$E_{fr} = \int_0^{H}\int_0^{\Delta x} u\left(\frac{\partial \tau_{xz}}{\partial z}\right) dx\,dz = \Delta x \int_0^{H} u\left(\frac{\Delta p}{\Delta x}\right) dz = -\frac{\Delta x}{12\mu}\left(\frac{\Delta p}{\Delta x}\right)^2 H^3. \tag{57}$$

For this steady, fully developed configuration, the pressure contribution E_{in} in Eq. (56) and the viscous-force contribution E_{fr} in Eq. (57) cancel in the mechanical-energy equation. There is consequently no net increase in the kinetic energy of the established velocity field. This cancellation is consistent with pressure work supplying the energy that is converted through viscous dissipation, subject to the stated no-slip boundaries and control-volume assumptions.

The mechanical-energy equation alone does not determine the subsequent thermal state. Reading the cancellation as destruction of energy would therefore be incorrect. The lost mechanical energy appears in the internal-energy balance, and its eventual disposition depends on heat conduction, thermal boundary conditions, and transport through the control-volume boundaries. The distinction is between conversion and disappearance of energy.

In physical terms, viscosity converts mechanical work into internal energy in the sheared flow. This conversion is represented by the dissipation function in Eq. (51) and

is included in the total-energy balance discussed around Eq. (53). A temperature rise is possible, but it is not determined by mechanical dissipation alone: the fluid may also transfer heat to its surroundings. The Poiseuille example therefore illustrates why the kinetic-energy equation and the thermal balance must be interpreted together.

7.3. Energy Transfer and Dissipation: In the Nonsliding Rigid Rotating Flow

Consider two material elements, e_1 and e_2, in the rotating configuration of Figure 16. Panel (a) shows their positions at $t = t_1$, and panel (b) shows their positions at $t = t_2$. The outer element travels a longer arc because its tangential speed is greater, but the distance between the two material points remains unchanged under exact rigid-body rotation. This is the defining kinematic distinction from deformation. White discusses this rigid-body character [37]. The subsequent comparison examines the stress and power expressions associated with the SST and the proposed AST for this same velocity field.

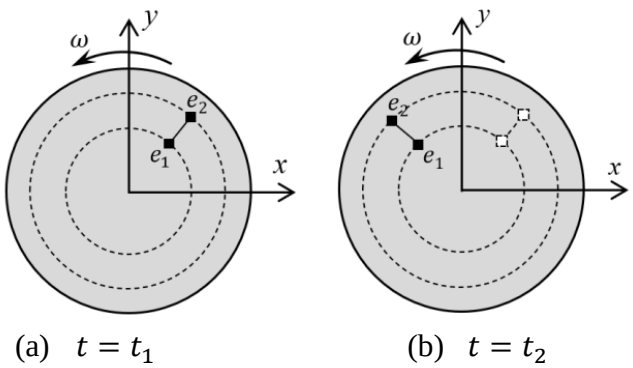


Figure 16. Material-Element Motion During Rigid-Body Rotation

Substitution of rigid-body rotation into the conventional Newtonian relation gives the zero viscous stresses in Eq. (28). Viscous stress power and viscous dissipation then vanish. The pressure field and the radial momentum balance remain necessary even though the viscous contribution is zero.

Section 3.5 introduces a loaded-cylinder scenario in which the author assumes nonzero torque transfer while retaining rigid-body rotation. The compatibility of those assumptions remains essential. The AST gives nonzero components for the prescribed rotating velocity field, whereas the SST gives zero viscous stress. The energy discussion must therefore examine the resulting mechanical and angular-momentum balances, not merely choose a definition that forces one part of the power expression to vanish.

7.3.1. Energy Dissipation on Friction Forces in a Rigid Rotating Flow: SST versus AST

For the symmetric tensor in two-dimensional polar coordinates, the viscous-force density is written as

$$\begin{cases} F_r^{vis} = \dfrac{\partial \tau_{rr}}{\partial r} + \dfrac{1}{r}\dfrac{\partial \tau_{r\theta}}{\partial \theta} + \dfrac{1}{r}(\tau_{rr} - \tau_{\theta\theta}), \\ F_\theta^{vis} = \dfrac{\partial \tau_{\theta r}}{\partial r} + \dfrac{1}{r}\dfrac{\partial \tau_{\theta\theta}}{\partial \theta} + \dfrac{2}{r}\tau_{\theta r}. \end{cases} \tag{58}$$

The zero viscous stresses in Eq. (28) give zero viscous-force density for exact rigid-body rotation under the symmetric Newtonian relation.

For comparison, the proposed AST is expressed in two-dimensional polar coordinates as follows; the appendix provides the adopted component calculation:

$$\vec{\vec{\tau}}^{asym} = \begin{bmatrix} \tau_{rr} & \tau_{r\theta} \\ \tau_{\theta r} & \tau_{\theta\theta} \end{bmatrix} = \begin{bmatrix} \mu \dfrac{\partial u_r}{\partial r} & \mu\left(\dfrac{1}{r}\dfrac{\partial u_r}{\partial \theta} - \dfrac{u_\theta}{r}\right) \\ \mu \dfrac{\partial u_\theta}{\partial r} & \mu\left(\dfrac{1}{r}\dfrac{\partial u_\theta}{\partial \theta} + \dfrac{u_r}{r}\right) \end{bmatrix}. \tag{59}$$

Here $\tau_{r\theta} = \mu(r^{-1}\partial u_r/\partial\theta - u_\theta/r)$ and $\tau_{\theta r} = \mu\partial u_\theta/\partial r$ are the unequal components in the proposed convention. Substituting the rigid-rotation velocity field gives

$$\vec{\vec{\tau}}^{asym} = \begin{bmatrix} 0 & -\mu\omega \\ \mu\omega & 0 \end{bmatrix}. \tag{60}$$

The corresponding divergence expressions, using the component convention in the appendix, are

$$\begin{cases} f_r^{vis} = \dfrac{\partial\tau_{rr}}{\partial r} + \dfrac{1}{r}\dfrac{\partial\tau_{r\theta}}{\partial\theta} + \dfrac{1}{r}(\tau_{rr} - \tau_{\theta\theta}), \\ f_\theta^{vis} = \dfrac{\partial\tau_{\theta r}}{\partial r} + \dfrac{1}{r}\dfrac{\partial\tau_{\theta\theta}}{\partial\theta} + \dfrac{1}{r}(\tau_{r\theta} + \tau_{\theta r}). \end{cases} \tag{61}$$

The formulas in Eqs. (58) and (61) are written for symmetric and nonsymmetric component sets, respectively. Their comparison requires consistent placement of the force-direction and surface-normal indices.

Applying the displayed AST divergence to the rigid-rotation field gives

$$\begin{cases} f_r^{vis} = 0, \\ f_\theta^{vis} = 0. \end{cases} \tag{62}$$

The author disputes the coordinate calculation in the critique [19] and argues that the divergence formula used there assumes symmetry. The present displayed calculation gives zero bulk viscous-force density for rigid-body rotation under the AST. This result addresses linear momentum only. A zero divergence does not establish zero torque, an admissible local angular-momentum balance, or a thermodynamically consistent stress-power expression. Those additional requirements must be assessed independently before drawing a conclusion about the physical acceptability of a nonsymmetric stress tensor.

7.3.2. Energy Transfer and Dissipation in Rigid Rotating Flows: SST versus AST

The analogy in Figure 17 is introduced to illustrate force transfer without sliding at a solid contact. Block M1 is fixed to a trolley, and block M2 rests on M1. A resisting force f acts on the trolley, while a force F acts on M2. Uniform translation of the complete system requires equal and opposite external forces, written as $F = -f$ in the selected one-dimensional sign convention. Static friction between the blocks transmits the applied load.

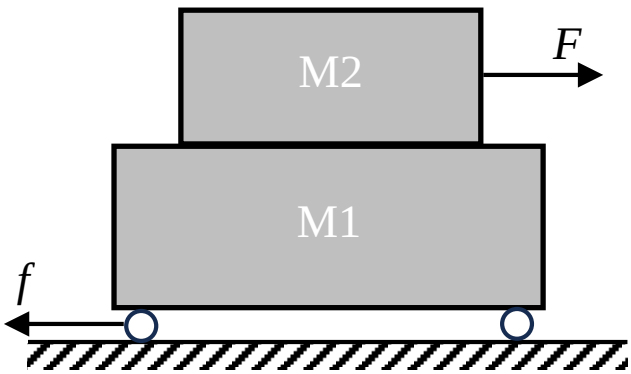


Figure 17. Force Transmission Through Static Contact Between Two Blocks

The author compares the static contact force between M1 and M2 with the proposed fluid stresses in a loaded rotating system. The intended similarities concern force transmission and the absence of relative sliding. The analogy is descriptive, however, and does not establish that an ordinary Newtonian fluid possesses the same constitutive response as a solid interface with static friction.

1) The two blocks have no relative sliding while static contact is maintained. The author compares this with preservation of material-point distances in rigid-body rotation. 2) The applied force and trolley resistance have equal magnitudes in steady translation; the interfacial static friction transmits the force from M2 to M1. This is compared with a proposed torque transfer from the outer cylinder to the inner cylinder. 3) The ideal nonsliding interface does not dissipate energy through relative motion, although it transmits mechanical power between bodies moving in the laboratory frame. These statements distinguish contact power transfer from dissipation at that interface.

4) Work supplied through the applied force can be transmitted through the block contact and dissipated at the location of the trolley resistance. The author compares this distribution with input torque at one cylinder and a resisting load at the other. 5) The required static contact force depends on the external loading and remains within the admissible static-friction range. In an ideal unloaded constant-speed case, no applied force is required and the contact need not carry a tangential load. The corresponding fluid analogy requires caution: a static-friction law can sustain a load without a rate of slip, whereas a Newtonian viscous law relates stress to deformation rate. The analogy therefore cannot determine the fluid stress without an explicit constitutive mechanism.

The proposed analogy motivates a distinction between power transmission and dissipation, but it does not resolve the constitutive compatibility of nonzero viscous torque and exact rigid-body rotation. That compatibility must be established using the governing balances and the selected material model.

The author next decomposes the AST stress-power expression and proposes assigning separate meanings to its terms. The algebraic identity can be examined directly, while the physical labels require additional justification.

Using the stress-work product rule discussed in [25,41], the AST expression is written as

$$W^{vis} = \frac{\partial(u_i \tau_{ij}^{asym})}{\partial x_j}. \tag{63}$$

The components τ_{ij}^{asym} denote the proposed asymmetric stress. Applying the product rule gives

$$W^{vis} = u_i \frac{\partial \tau_{ij}^{asym}}{\partial x_j} + \tau_{ij}^{asym} \frac{\partial u_i}{\partial x_j}. \tag{64}$$

The first term on the right-hand side of Eq. (64) is viscous-force power. For the rigid-rotation field, the displayed AST divergence is zero, so this term vanishes. The same bulk force-power result is obtained with the SST for that field. This agreement does not determine the remaining contraction or the boundary stress-power flux.

The second term in Eq. (64) is the contraction of the AST with the velocity gradient. In the conventional symmetric Newtonian model, the analogous contraction is interpreted as viscous dissipation [5,22,41]. For a nonsymmetric stress, that interpretation cannot simply be carried over without examining the complete constitutive and angular-momentum framework. In particular, the AST can give a nonzero contraction during rigid-body rotation. The source manuscript treats this as motivation to redefine dissipation, but the unchanged total stress-power identity still has to be satisfied.

Couette flow illustrates why zero bulk viscous-force density is not equivalent to zero viscous dissipation. In steady simple shear, the stress can be spatially uniform, so its divergence vanishes, while the deformation rate and viscous heating remain nonzero [25]. Mechanical power enters through moving boundaries. The author uses the term sliding to describe the relative deformation and compares it with frictional motion between solid objects. The comparison is useful only when the different constitutive laws and the dimensions of the power terms remain explicit.

To separate the proposed deformation-related and remaining contributions, the author rewrites the second term using the following algebraic identity:

$$\tau_{ij}^{asym}\frac{\partial u_i}{\partial x_j} = \tau_{ij}^{asym}\left(\frac{\partial u_i}{\partial x_j} + \frac{\partial u_j}{\partial x_i}\right) - \tau_{ij}^{asym}\frac{\partial u_j}{\partial x_i}. \tag{65}$$

The source manuscript assigns the following physical interpretations to the terms in this decomposition:

1) The proposed alternative dissipation function is defined as

$$\Phi = \tau_{ij}^{asym}\left(\frac{\partial u_i}{\partial x_j} + \frac{\partial u_j}{\partial x_i}\right). \tag{66}$$

The symmetric velocity-gradient combination in brackets vanishes for rigid-body rotation. The proposed expression therefore gives zero for that velocity field even if the AST itself is nonzero. The author interprets this as a description of dissipation controlled by deformation rather than by the mere existence of stress. However, a chosen term that vanishes in one flow is not, by itself, a complete thermodynamic derivation. The remaining term and the full mechanical-power balance must also be interpreted consistently, and the definition must satisfy the relevant material-frame and angular-momentum requirements.

2) The remaining term in Eq. (65) is $-\tau_{ij}^{asym}\partial u_j/\partial x_i$. Its dimensions are power per unit volume, not energy. The author proposes interpreting it as internal power transfer and draws an analogy with reactive power in electrical circuits. That analogy does not establish a mechanical flux: a physical transfer term must be connected to boundary power or an explicitly defined local flux in the energy balance. For the rigid-rotation field, the proposed term evaluates to

$$-\tau_{ij}^{asym}\frac{\partial u_j}{\partial x_i} = -\tau_{r\theta}^{asym}\frac{\partial u_\theta}{\partial r} - \tau_{\theta r}^{asym}\left(\frac{1}{r}\frac{\partial u_r}{\partial \theta} - \frac{u_\theta}{r}\right) = 2\mu\omega^2, \tag{67}$$

Integrating the proposed power-density term over the annular fluid region gives

$$E_{transfer} = \int_{R_1}^{R_2} 2\mu\omega^2\, 2\pi r\, dr = 2\pi\mu\omega^2(R_2^2 - R_1^2). \tag{68}$$

The calculation uses unit axial length and inner and outer radii R_1 and R_2, as shown in Figure 10. The author associates the quantities $2\pi\mu\omega^2 R_2^2$ and $2\pi\mu\omega^2 R_1^2$ with outer and inner boundary powers. Their difference is nonzero when the radii differ. A consistent interpretation must therefore account for that difference through the total-energy and angular-momentum balances; labeling it transfer alone does not establish conservation in the proposed loaded steady state.

A complete power-transfer interpretation would also need to identify the torque associated with each boundary traction and its orientation. In a steady annular control volume, unequal mechanical powers at equal angular speed imply unequal torques unless another contribution is present. If the proposed tensor carries a local antisymmetric part, that part enters the angular-momentum accounting and cannot be ignored because the bulk linear-momentum divergence happens to vanish. Generalized continua can include internal rotations and couple stresses, but those descriptions introduce additional fields and balances. They cannot be inferred from the scalar power term alone. The present decomposition is therefore best treated as a proposed interpretation awaiting that complete framework. The electrical analogy illustrates that transfer and dissipation are different ideas, but it does not identify the mechanical storage, flux, or angular-momentum pathway required here. Establishing that pathway would make the rotating-cylinder comparison testable on its own terms rather than relying on the assumption that all boundary power differences must represent nondissipative transfer.

8. Energy Dissipation in Compressible Flows: Via AST

Section 7 introduces the alternative expression in Eq. (66) and its proposed interpretation. This section applies that expression to the complete AST, including the volumetric contribution. The calculation is an assessment of the proposed definition; it should be distinguished from a derivation establishing that the expression is the thermodynamic dissipation of an ordinary Newtonian fluid.

To include the volumetric term, the complete viscous-stress tensor replaces the tensor used in the preceding expression, giving

$$\sigma_{ij}^{asym} = \tau_{ij}^{asym} + \frac{1}{3}\mu(\nabla \cdot \vec{V})\delta_{ij} = \mu\left(\frac{\partial u_i}{\partial x_j}\right) + \frac{\mu}{3}\left(\frac{\partial u_k}{\partial x_k}\right)\delta_{ij}. \tag{69}$$

Substituting the proposed component relations gives

$$\begin{aligned}\Phi &= \sigma_{ij}\left(\frac{\partial u_i}{\partial x_j} + \frac{\partial u_j}{\partial x_i}\right) \\ &= \mu\left\{2\left[\left(\frac{\partial u}{\partial x}\right)^2 + \left(\frac{\partial v}{\partial y}\right)^2 + \left(\frac{\partial w}{\partial z}\right)^2\right] + \left(\frac{\partial u}{\partial y} + \frac{\partial v}{\partial x}\right)^2 + \left(\frac{\partial w}{\partial y} + \frac{\partial v}{\partial z}\right)^2 + \right. \\ &\qquad \left.\left(\frac{\partial u}{\partial z} + \frac{\partial w}{\partial x}\right)^2 + \frac{1}{3}\left(\frac{\partial u}{\partial x} + \frac{\partial v}{\partial y} + \frac{\partial w}{\partial z}\right)^2\right\}.\end{aligned} \tag{70}$$

The resulting expression differs from Eq. (33) in the coefficient multiplying the squared velocity divergence. The author emphasizes that this coefficient is positive in the proposed representation. Nevertheless, comparison of individual coefficients is insufficient to establish physical admissibility: the complete constitutive relation and stress-power balance must be examined. For the isotropic dilatational field already considered in Eq. (35), the velocity-gradient conditions are

$$\frac{\partial u}{\partial x} = \frac{\partial v}{\partial y} = \frac{\partial w}{\partial z} = \varepsilon \neq 0 \quad \text{and} \quad \frac{\partial u_i}{\partial x_j} = 0 \quad \text{for } i \neq j. \tag{71}$$

For this field, the proposed expression evaluates to

$$\Phi = \mu\left(2 \times 3\varepsilon^2 + \frac{1}{3} \times 9\varepsilon^2\right) = 9\mu\varepsilon^2. \tag{72}$$

The positive result follows algebraically from the proposed definition and selected coefficient. It does not prove that the zero value under Stokes' hypothesis was inconsistent, nor that an AST is necessary to obtain dilatational dissipation. In the conventional symmetric formulation, a nonzero bulk viscosity supplies such a contribution.

9. Conclusions

This manuscript compares the conventional symmetric viscous-stress description with the author's proposed asymmetric relation through momentum, wall-traction, sphere-flow, and energy examples. The original objections concern spatial stress increments, grid dependence, complementary shear components, rigid-body rotation, and compressible dissipation. Several of these objections depend on assumptions that must be stated separately from local stress symmetry. In particular, equality at a common point does not imply equality at different positions, and a complementary tensor component is not automatically an additional traction on the same physical surface. The proposed AST calculations are retained to make the comparison explicit, but they do not establish a general failure of the symmetric Newtonian model.

The following points summarize the proposed formulation and the conditions that remain necessary for its assessment:

1) The AST is motivated by extending the simple-shear viscosity relation to individual velocity-gradient components. This extension is a constitutive proposal, not a consequence free of material assumptions. 2) The momentum divergence can reproduce a familiar Cartesian viscous term under the stated coefficient choices. Agreement of a bulk equation does not establish equality of boundary tractions or torques. 3) The fluid-versus-solid deformation comparison distinguishes viscous and elastic response, but both materials remain subject to angular-momentum balance.

4) The spatial-increment and Poiseuille examples require local component equality to be separated from equalities between different positions. A symmetric, spatially varying stress field is mathematically admissible. 5) The airfoil and sphere examples must use traction on the actual boundary and the correct dimensional surface integration; the sphere's net transverse force vanishes by axisymmetry. 6) The loaded-cylinder example requires a compatible velocity field and constitutive law. Exact rigid-body rotation of an ordinary Newtonian fluid has zero viscous stress, although pressure is nonzero. 7) The proposed energy decomposition is an algebraic identity whose transfer and dissipation labels require independent physical justification. 8) The zero dissipation of isotropic dilation under Stokes' hypothesis reflects its zero-bulk-viscosity assumption; positive bulk viscosity can be included within a symmetric stress model.

The central unresolved task is to specify a complete constitutive framework for the proposed nonsymmetric stress, including angular-momentum transport, observer invariance, boundary traction, and thermodynamic admissibility. If internal rotations, couple stresses, or body couples are intended, their governing variables and balance laws must be supplied. Without that framework, the examples provide a statement of the author's proposal and its contested interpretations rather than a demonstrated replacement for classical Newtonian fluid mechanics.

The scope of the conclusion is therefore theoretical. No experimental force measurement, torque measurement, temperature record, or numerical refinement dataset is supplied to adjudicate the proposed alternatives. A future test would need observables for which the two complete models make different predictions under the same boundary conditions, together with independently specified material properties. Such a comparison should distinguish uncertainty in measured viscosity from uncertainty in the constitutive form. It should also distinguish a disagreement caused by coordinate indexing or surface integration from a genuine physical difference. The appendix is included to expose the adopted coordinate calculations, but a component derivation must remain consistent with the tensor convention used throughout the main text. The retained examples identify where the author's proposed description differs from the conventional one and where additional justification is required. They should not be described as establishing that all classical symmetric-stress calculations are coincidentally correct or that every apparent difficulty has already been resolved by the AST.

Competing Interests

The author declares no competing interests.

Data Availability

This manuscript presents theoretical arguments and mathematical derivations.

Funding

This research received no external funding.

References

[1] Masuda, S. (2012). The study of mathematical history on the equations of Navier-Stokes and Boltzmann as the microscopically-descriptive hydrodynamic equations. *RIMS Kōkyūroku, 1776*, 75–90.

[2] Anderson, J. D. (2011). *Fundamentals of Aerodynamics* (5th ed.). McGraw-Hill.

[3] Bertin, J. J., & Cummings, R. M. (2013). *Aerodynamics for Engineers* (6th ed.). Pearson.

[4] White, F. M. (2009). *Fluid Mechanics*. McGraw-Hill.

[5] Kundu, P. K., Cohen, I. M., Dowling, D. R., & Capecelatro, J. (2025). *Fluid Mechanics* (7th ed.). Academic Press.
[6] Schlichting, H., & Gersten, K. (2017). *Boundary-Layer Theory* (9th ed.). Springer.
[7] Hibbeler, R. C. (2021). *Fluid Mechanics in SI Units* (2nd ed.). Pearson.
[8] Le Méhauté, B. (1976). *An Introduction to Hydrodynamics and Water Waves*. Springer-Verlag.
[9] Condiff, D. W., & Dahler, J. S. (1964). Fluid mechanical aspects of antisymmetric stress. *The Physics of Fluids, 7*(6), 842–854.
[10] Aero, E. L., Bulygin, A. N., & Kuvshinskii, E. V. (1965). Asymmetric hydromechanics. *Journal of Applied Mathematics and Mechanics, 29*(2), 333–346.
[11] Listrov, A. T. (1967). Model of a viscous fluid with an antisymmetric stress tensor. *Journal of Applied Mathematics and Mechanics, 31*(1), 115–119.
[12] Van D'en, N., & Listrov, A. T. (1967). Nonisothermal model of asymmetric fluids. *Fluid Dynamics, 2*(5), 87–89.
[13] Lilly, D. K. (1967). The representation of small-scale turbulence in numerical simulation experiments. In *Proceedings of the IBM Scientific Computing Symposium on Environmental Sciences* (pp. 195–210). IBM.
[14] Kim, J., & Leonard, A. (2024). The early days and rise of turbulence simulation. *Annual Review of Fluid Mechanics, 56*, 21–44.
[15] Saffman, P. G. (1970). A model for inhomogeneous turbulent flow. *Proceedings of the Royal Society of London. Series A, Mathematical and Physical Sciences, 317*(1530), 417–433.
[16] Hanjalić, K., & Launder, B. E. (1972). A Reynolds stress model of turbulence and its application to thin shear flows. *Journal of Fluid Mechanics, 52*(4), 609–638.
[17] Launder, B. E., & Spalding, D. B. (1974). The numerical computation of turbulent flows. *Computer Methods in Applied Mechanics and Engineering, 3*(2), 269–289.
[18] Sheng, W. (2020). A revisit of Navier–Stokes equation. *European Journal of Mechanics - B/Fluids, 80*, 60–71.
[19] Natarajan, G., & Natarajan, M. (2021). Critique on "A revisit of Navier–Stokes equation". *European Journal of Mechanics - B/Fluids, 85*, 21–23.
[20] Luo, J. (2024). More considerations about the symmetry of the stress tensor of fluids. *The Journal of Chemical Physics, 161*(4), Article 044112.
[21] Sheng, W. (2026). *On fluid stress tensor: Is symmetric stress tensor correct for fluids?* [Manuscript]. ResearchGate. https://www.researchgate.net/publication/410895675_On_Fluid_Stress_Tensor_Is_Symmetric_Stress_Tensor_Correct_for_Fluids
[22] Anderson, J. D. (2017). *Fundamentals of Aerodynamics* (6th ed.). McGraw-Hill Education.
[23] Houghton, E. L., Carpenter, P. W., Collicott, S. H., & Valentine, D. T. (2017). *Aerodynamics for Engineering Students* (7th ed.). Butterworth-Heinemann.
[24] Çengel, Y. A., & Cimbala, J. M. (2018). *Fluid Mechanics: Fundamentals and Applications* (4th ed.). McGraw-Hill Education.
[25] Anderson, J. D. (2024). *Fundamentals of Aerodynamics* (7th ed.). McGraw Hill.
[26] Newman, J. N. (2017). *Marine Hydrodynamics* (40th anniversary ed.). MIT Press.
[27] Witherden, F. D., & Jameson, A. (2017). Future directions of computational fluid dynamics. In *23rd AIAA Computational Fluid Dynamics Conference* (Paper No. 2017-3791). American Institute of Aeronautics and Astronautics.
[28] Spalart, P. R., & Venkatakrishnan, V. (2016). On the role and challenges of CFD in the aerospace industry. *The Aeronautical Journal, 120*(1223), 209–232.
[29] Stokes, G. G. (1851). On the effect of the internal friction of fluids on the motion of pendulums. *Transactions of the Cambridge Philosophical Society, 9*, 8–106.
[30] Sutterby, J. L. (1973). Falling sphere viscometer. *Journal of Physics E: Scientific Instruments, 6*(10), 1001–1005.
[31] Cartwright, J. H. E. (2020). Stokes' law, viscometry, and the Stokes falling sphere clock. *Philosophical Transactions of the Royal Society A: Mathematical, Physical and Engineering Sciences, 378*(2179), Article 20200214.
[32] Millikan, R. A. (1910). The isolation of an ion, a precision measurement of its charge, and the correction of Stokes's law. *Science, 32*(822), 436–448.
[33] Stokes, G. G. (1845). On the theories of the internal friction of fluids in motion, and of the equilibrium and motion of elastic solids. *Transactions of the Cambridge Philosophical Society, 8*, 287–319.
[34] White, F. M., & Majdalani, J. (2022). *Viscous Fluid Flow* (4th ed.). McGraw Hill.
[35] Kurzweg, U. H. (2003, November). *Derivation of the Stokes Drag Formula*. University of Florida. https://web.mae.ufl.edu/uhk/STOKES-DRAG-FORMULA.pdf
[36] Lautrup, B. (2005). *Physics of Continuous Matter: Exotic and Everyday Phenomena in the Macroscopic World*. Institute of Physics Publishing.
[37] White, F. M. (2016). *Fluid Mechanics* (8th ed.). McGraw-Hill Education.
[38] Dimotakis, P. E., & Candler, G. V. (2014, June 2–5). *Energy transformation, transfer, and release dynamics in high-speed turbulent flows* [Conference presentation]. Basic Combustion Research Review, Washington, DC, United States. https://community.apan.org/cfs-file/__key/telligent-evolution-components-attachments/13-7784-00-00-00-13-54-76/Dimotakis_2D00_Candler.pdf
[39] Yang, X., Xiao, G., Du, Y., Liu, L., Wei, D., & Gui, Y. (2021). Heat transfer with interface effects in high-enthalpy and high-speed flow: Modelling review and recent progress. *Applied Thermal Engineering, 195*, Article 116721.
[40] Potter, M. C., & Wiggert, D. C. (2025). *Applied Fluid Mechanics* (6th ed.). Springer.
[41] White, F. M. (2006). *Viscous Fluid Flow* (3rd ed.). McGraw-Hill Higher Education.

Appendix

Asymmetric Shear Stresses in Polar Coordinates

The Cartesian and polar coordinates in Figure A1 are related by

$$x = r\cos\theta;\ y = r\sin\theta, \tag{A1}$$

The corresponding unit-vector relations are

$$\vec{e}_r = \vec{i}\cos\theta + \vec{j}\sin\theta;\ \vec{e}_\theta = -\vec{i}\sin\theta + \vec{j}\cos\theta, \tag{A2}$$

The vectors $\vec{e}_r$ and $\vec{e}_\theta$ point in the radial and tangential directions. Unlike the Cartesian basis vectors $\vec{i}$ and $\vec{j}$, their directions vary with the angular coordinate. Their derivatives must therefore be retained when differentiating vector and tensor fields.

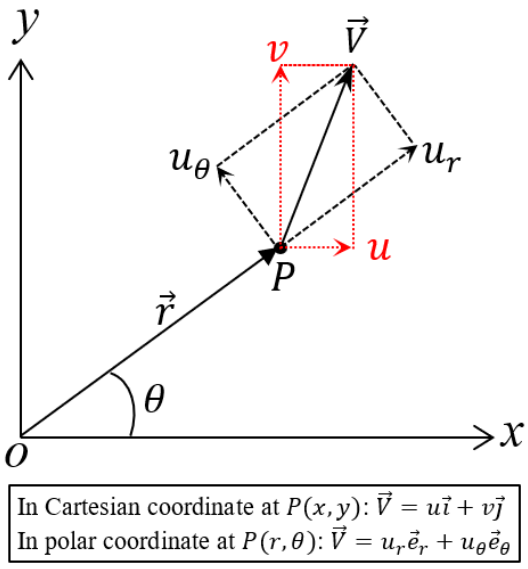


Figure A1. Cartesian and Polar Coordinate Bases

Differentiation of the polar basis vectors with respect to r and θ gives

$$\frac{\partial\vec{e}_r}{\partial r} = 0;\ \frac{\partial\vec{e}_\theta}{\partial r} = 0;\ \frac{\partial\vec{e}_r}{\partial\theta} = \vec{e}_\theta;\ \frac{\partial\vec{e}_\theta}{\partial\theta} = -\vec{e}_r. \tag{A3}$$

Applying the chain rule to the coordinate transformation gives

$$\begin{cases} \dfrac{\partial}{\partial r} = \dfrac{\partial}{\partial x}\dfrac{\partial x}{\partial r} + \dfrac{\partial}{\partial y}\dfrac{\partial y}{\partial r} = \cos\theta\dfrac{\partial}{\partial x} + \sin\theta\dfrac{\partial}{\partial y}, \\ \dfrac{\partial}{\partial\theta} = \dfrac{\partial}{\partial x}\dfrac{\partial x}{\partial\theta} + \dfrac{\partial}{\partial y}\dfrac{\partial y}{\partial\theta} = -r\sin\theta\dfrac{\partial}{\partial x} + r\cos\theta\dfrac{\partial}{\partial y}. \end{cases} \tag{A4}$$

Combining Eqs. (A2) and (A4) yields the gradient operator

$$\nabla = \vec{e}_r\frac{\partial}{\partial r} + \vec{e}_\theta\frac{1}{r}\frac{\partial}{\partial\theta} = \vec{i}\frac{\partial}{\partial x} + \vec{j}\frac{\partial}{\partial y}. \tag{A5}$$

In the appendix's dyadic convention, the unsymmetrized velocity-gradient expression is

$$\begin{aligned} \vec{\vec{\varepsilon}} = \nabla\vec{V} &= \left(\vec{e}_r\frac{\partial}{\partial r} + \vec{e}_\theta\frac{1}{r}\frac{\partial}{\partial\theta}\right)(\vec{e}_r u_r + \vec{e}_\theta u_\theta) \\ &= \left(\frac{\partial u_r}{\partial r}\right)(\vec{e}_r\vec{e}_r) + \left(\frac{1}{r}\frac{\partial u_r}{\partial\theta} - \frac{u_\theta}{r}\right)(\vec{e}_\theta\vec{e}_r) + \left(\frac{\partial u_\theta}{\partial r}\right)(\vec{e}_r\vec{e}_\theta) + \left(\frac{1}{r}\frac{\partial u_\theta}{\partial\theta} + \frac{u_r}{r}\right)(\vec{e}_\theta\vec{e}_\theta), \end{aligned} \tag{A6}$$

Double arrows denote a tensor, while products such as $\vec{e}_r\vec{e}_\theta$ denote dyadic basis elements. The quantity in Eq. (A6) is an unsymmetrized velocity gradient, not the conventional symmetric rate-of-strain tensor. The source manuscript assigns its components as follows; the ordering must be used consistently with the stress and divergence definitions:

$$\varepsilon_{rr} = \frac{\partial u_r}{\partial r};\ \varepsilon_{r\theta} = \frac{1}{r}\frac{\partial u_r}{\partial \theta} - \frac{u_\theta}{r};\ \varepsilon_{\theta r} = \frac{\partial u_\theta}{\partial r};\ \varepsilon_{\theta\theta} = \frac{1}{r}\frac{\partial u_\theta}{\partial \theta} + \frac{u_r}{r}. \tag{A7}$$

For the proposed asymmetric constitutive relation, the polar-coordinate matrix is written as

$$\vec{\vec{\tau}} = \mu \begin{bmatrix} \dfrac{\partial u_r}{\partial r} & \dfrac{1}{r}\dfrac{\partial u_r}{\partial \theta} - \dfrac{u_\theta}{r} \\ \dfrac{\partial u_\theta}{\partial r} & \dfrac{1}{r}\dfrac{\partial u_\theta}{\partial \theta} + \dfrac{u_r}{r} \end{bmatrix}. \tag{A8}$$

The viscous-force density $\vec{f}^{vis}$ is expressed as the divergence of the adopted stress tensor:

$$\vec{f}^{vis} = \nabla \cdot \vec{\vec{\tau}}. \tag{A9}$$

Applying the polar-coordinate differential operator to the expression associated with Eq. (A8) gives

$$\begin{aligned} \vec{f}^{vis} = \nabla \cdot \vec{\vec{\tau}} = \left(\vec{e}_r\frac{\partial}{\partial r} + \vec{e}_\theta\frac{1}{r}\frac{\partial}{\partial \theta}\right) \cdot \Bigg\{ \mu \Bigg[& \left(\frac{\partial u_r}{\partial r}\right)(\vec{e}_r\vec{e}_r) + \left(\frac{1}{r}\frac{\partial u_r}{\partial \theta} - \frac{u_\theta}{r}\right)(\vec{e}_\theta\vec{e}_r) \\ & + \left(\frac{\partial u_\theta}{\partial r}\right)(\vec{e}_r\vec{e}_\theta) + \left(\frac{1}{r}\frac{\partial u_\theta}{\partial \theta} + \frac{u_r}{r}\right)(\vec{e}_\theta\vec{e}_\theta) \Bigg] \Bigg\} \\ = \mu \left[\frac{\partial \varepsilon_{rr}}{\partial r} + \frac{1}{r}\frac{\partial \varepsilon_{r\theta}}{\partial \theta} + \frac{1}{r}(\varepsilon_{rr} - \varepsilon_{\theta\theta})\right]\vec{e}_r & + \mu \left[\frac{\partial \varepsilon_{\theta r}}{\partial r} + \frac{1}{r}\frac{\partial \varepsilon_{\theta\theta}}{\partial \theta} + \frac{1}{r}(\varepsilon_{r\theta} + \varepsilon_{\theta r})\right]\vec{e}_\theta. \end{aligned} \tag{A10}$$

The displayed radial and tangential force-density components are therefore

$$\begin{cases} f_r^{vis} = \mu \left[\dfrac{\partial \varepsilon_{rr}}{\partial r} + \dfrac{1}{r}\dfrac{\partial \varepsilon_{r\theta}}{\partial \theta} + \dfrac{1}{r}(\varepsilon_{rr} - \varepsilon_{\theta\theta})\right], \\ f_\theta^{vis} = \mu \left[\dfrac{\partial \varepsilon_{\theta r}}{\partial r} + \dfrac{1}{r}\dfrac{\partial \varepsilon_{\theta\theta}}{\partial \theta} + \dfrac{1}{r}(\varepsilon_{r\theta} + \varepsilon_{\theta r})\right]. \end{cases} \tag{A11}$$

Substituting the component expressions from Eq. (A8) into Eq. (A11) gives the following radial and tangential formulas. Their use requires a consistent convention for the tensor indices and the contracted index in the divergence:

$$\begin{cases} f_r^{vis} = \mu \left[\dfrac{1}{r}\dfrac{\partial}{\partial r}\left(r\dfrac{\partial u_r}{\partial r}\right) + \dfrac{1}{r^2}\dfrac{\partial^2 u_r}{\partial \theta^2} - \dfrac{2}{r^2}\dfrac{\partial u_\theta}{\partial \theta} - \dfrac{u_r}{r^2}\right], \\ f_\theta^{vis} = \mu \left[\dfrac{1}{r}\dfrac{\partial}{\partial r}\left(r\dfrac{\partial u_\theta}{\partial r}\right) + \dfrac{1}{r^2}\dfrac{\partial^2 u_\theta}{\partial \theta^2} + \dfrac{2}{r^2}\dfrac{\partial u_r}{\partial \theta} - \dfrac{u_\theta}{r^2}\right]. \end{cases} \tag{A12}$$